8-2009

Chameleon Coatings: Adaptive Surfaces to Reduce Friction and Wear in Extreme Environments

Christopher Muratore
University of Dayton, cmuratore1@udayton.edu

Andrey A. Voevodin
Air Force Research Laboratory

Chameleon Coatings: Adaptive Surfaces to Reduce Friction and Wear in Extreme Environments

C. Muratore and A.A. Voevodin

Thermal Science and Materials Branch, Air Force Research Laboratory, Wright-Patterson Air Force Base, Ohio 45433; email: chris.muratore@wpafb.af.mil

Annu. Rev. Mater. Res. 2009. 39:297–324

First published online as a Review in Advance on April 7, 2009

The *Annual Review of Materials Research* is online at matsci.annualreviews.org

This article's doi: 10.1146/annurev-matsci-082908-145259

1531-7331/09/0804-0297$20.00

Key Words

tribology, high temperature, aerospace, surface analysis, electron microscopy

Abstract

Adaptive nanocomposite coating materials that automatically and reversibly adjust their surface composition and morphology via multiple mechanisms are a promising development for the reduction of friction and wear over broad ranges of ambient conditions encountered in aerospace applications, such as cycling of temperature and atmospheric composition. Materials selection for these composites is based on extensive study of interactions occurring between solid lubricants and their surroundings, especially with novel in situ surface characterization techniques used to identify adaptive behavior on size scales ranging from 10^{-10} to 10^{-4} m. Recent insights on operative solid-lubricant mechanisms and their dependency upon the ambient environment are reviewed as a basis for a discussion of the state of the art in solid-lubricant materials.

FUNDAMENTALS OF SOLID LUBRICATION IN DIVERSE ENVIRONMENTS

Tribology: the study of surfaces in relative motion, from the Greek word tribos, meaning rubbing

Friction coefficient: the ratio of tangential force to applied normal force, or the ratio of shear strength to pressure if both forces are divided by contact area

Abrasive wear: the plowing away of softer material by harder particles at contact interfaces

Adhesive wear: asperities from both surfaces in contact adhere, and material from the softer surface is sheared away as the counterface moves

Fatigue wear: the removal of material due to crack growth and propagation over repeated load cycles

Wear rate: the rate of material loss from a surface due to sliding contact, often reported in units of volume lost per unit sliding distance per unit of applied normal force (e.g., $mm^3\ m^{-1}\ N^{-1}$)

A spray of liquid lubricant from a can available at the hardware store solves most familiar friction and wear problems on Earth under ordinary conditions of ambient pressure, humidity, and temperature. When any one of those operating parameters reaches the limits of advanced engineering materials, however, the availability of suitable lubricants is diminished significantly. Moreover, if operation throughout a broad range of any one of these environmental factors is desired, the number of choices becomes exactly zero; tribologists have found that no single surface can lubricate effectively outside a narrow span of ambient humidity or temperature (1–3). In fact, one of the primary technological barriers for the development of new jet engines for sustained high-mach-number (>5) flights and other key aerospace advances is the ability to lubricate mechanical assemblies from ambient temperature to >1000°C. Only recently have discoveries of self-adaptive mechanisms and subsequent developments in tribological coatings, made possible with modern instrumentation and pioneering efforts to observe phenomena at atomic through microscopic size scales at contact interfaces, illuminated potential avenues for lubrication over the temperature range of interest. These techniques are highlighted as the development of adaptive tribological coatings for use in extreme environments is reviewed.

Introduction to Solid Lubrication

The liquid lubricant that comes in a spray can fights friction between sliding contacts in a few ways, but primarily by velocity accommodation between surfaces in relative motion by shearing of the oil molecules across the solid-liquid-solid interface on the freshly sprayed parts. Most liquid lubricants that operate on this principle will volatilize in vacuum or elevated temperatures, which can lead to failure of not only the lubricated component, but also distant, unrelated components if the vapor from the liquid condenses or reacts on their surfaces (4, 5). Furthermore, decomposition products of oils at elevated temperatures can build up at interfaces and inhibit lubrication effects in a process referred to as coking (6). Solid lubricants are therefore employed in applications that are expected to operate in extremes of ambient pressure (such as the vacuum of space) or temperature, because their vapor pressure is ordinarily sufficiently low that sublimation does not contribute to their degradation while in use. For most applications, qualification of a material as a useful solid lubricant requires a reduction of the friction coefficient (the ratio of the shear stress of the contact surface to the applied normal load) in its presence to a value of <0.1 to 0.2. If the friction coefficient is higher, irreversible deformation of the contact surfaces is likely to occur (7, pp. 81–85; 8, 9). The rate at which the material is removed from a friction contact is also important. Wear from sliding contacts generally occurs through one or more of the following modes: abrasive wear, in which a hard counterface plows grooves into a softer surface; adhesive wear, in which material is taken away as it literally adheres to a counterface in relative motion; and/or fatigue wear, in which repeated stressing of a surface results in subsurface fracture and removal of material (10). Wear rates are typically quantified in terms of the volume of material removed by the opposing surface in contact with the solid lubricant (or counterface), normalized by the load and the total distance traversed on the solid-lubricant surface by the wear counterpart. A solid lubricant is considered to have moderate wear resistance if it demonstrates a wear rate between 10^{-6} and $10^{-5}\ mm^3\ N^{-1}\ m^{-1}$. The lower limit of solid-lubricant wear rates is $\approx 10^{-11}\ mm^3\ N^{-1}\ m^{-1}$ (11). As a reference to the reader, a wear rate of $1 \times 10^{-7}\ mm^3\ N^{-1}\ m^{-1}$ represents an average removal rate of less than 1 atomic layer per 1-cm pass of a counterpart with a 5-N load. Singer et al. (12) point out that even at this relatively low wear rate, the cylinder lining of an automobile engine

block would cease to allow sufficient compression after fewer than 100 miles of ordinary driving, suggesting that liquid lubrication should be selected if the application allows. Wear rates are often nonlinear. For example, sputtered coatings of MoS_2 with a particular microstructure demonstrate rapid wear over the first few thousand sliding cycles but then maintain very low wear rates for up to millions of cycles (13). Most of the adaptive coatings reviewed here rely on mechanisms activated by the wear process and therefore undergo brief periods of high wear as ambient conditions change. Because of the dynamic nature of wear, sometimes a more meaningful steady-state wear rate, which is measured only after the surfaces in the friction contact have stabilized in terms of their morphology and composition, is reported. The onset of the steady-state wear regime is best identified with an in situ measurement technique during wear tests, as described below.

Slippery solids fall into one of two categories: intrinsic lubricants, with an atomic structure near the surface that shears easily to facilitate interfacial sliding, or extrinsic lubricants, which require the influence of an additive provided by the surroundings to activate a shear mechanism. The development of coatings that can adapt from terrestrial air (with water vapor present) to space, or from ambient temperature to 1000°C in air, requires a thorough understanding of both types of lubrication. The intent of the remainder of this section is not to give a detailed review of single-phase solid lubricants but to provide sufficient information to prepare the reader to better understand some of the mechanisms occurring in adaptive composite materials related to those occurring in common, single-phase lubricants. Only those mechanisms operative in adaptive coatings are discussed in the context of seminal works from the past combined with more recent works.

Intrinsic lubricant: a lubricant that demonstrates low shear with no influence from its surroundings (i.e., vacuum)

Extrinsic lubricant: a lubricant that requires an additive from the ambient environment (e.g., water vapor) to provide low shear

Transition-metal dichalcogenides (TMD): materials such as MoS_2 that possess a layered atomic structure with weak chemical bonding between layers

Intrinsic Solid Lubricants

Examples of intrinsic lubricants include soft metals such as Au or Pb and transition-metal dichalcogenides (TMDs) such as MoS_2 and WS_2—all of which have a low shear strength [$\tau = 1$–2 MPa (14)] in the absence of significant concentrations of surrounding molecules (i.e., in vacuum). MoS_2 is the most commonly used intrinsic solid lubricant, and many comprehensive studies and reviews of its properties and performance have been published over the past 40 years (10, 15–18). In its sputter-deposited thin-film form, MoS_2 has a combination of properties that are difficult to match (8) but atomic-scale mechanisms that have been hard to uncover because of the difficulty associated with analyzing buried contact interfaces. Before the advent of sputter deposition, MoS_2 coatings were applied by burnishing powders on surfaces or by spraying suspensions of solid particles in solvent (19). Regardless of the application technique, the anisotropy of the hexagonal MoS_2 crystal gives rise to its easy-shear surface, wherein stacks of S-Mo-S planes, possessing strong, covalent in-plane bonding but weaker van der Waals bonding between atomic sheets, allow easy shear of atomic planes. Although easy shear occurs only between basal planes, the material need not start with its basal planes oriented parallel to the surface [that is, with preferential (002) crystalline orientation] because the atomic planes will self-align in the friction contact via one of the two microstructurally dependent mechanisms shown in **Figure 1**.

MoS_2 coatings of low relative density are commonly composed of freestanding columnar grains or platelets with a 50–500 nm diameter and a length comparable to the thickness of the film. These platelets grow naturally after deposition of a 5–20-nm-thick film of (002)-oriented material adjacent to the coating substrate interface (18, 20). The platelets generally comprise S-Mo-S planes oriented perpendicular to the substrate [that is, in the (100) orientation]; the exposed edges of these atomic planes yield a high surface energy (25,000 mJ m^{-2}) (21) and adhere well to contacting surfaces (8). Rapid wear occurs early in the life of the coating material by deformation of these long grains that remain in the wear track, where they are bent 90°, reorienting the (002)

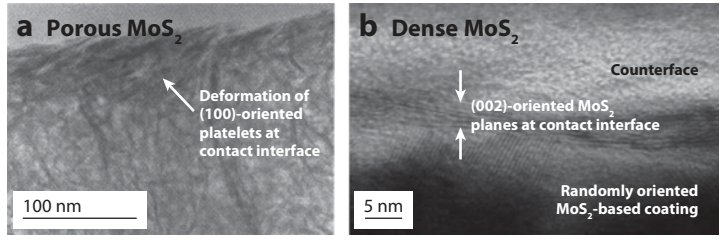

Figure 1

The response of MoS_2 coatings to rubbing exhibits a microstructural dependency. (*a*) Porous hexagonal MoS_2 composed of platelets with (100) orientation deforms under contact to reorient the platelets such that the (002) MoS_2 planes are parallel to the surface. Micrograph used with permission of the publisher and authors of Reference 20. (*b*) For a randomly oriented dense MoS_2-based coating, realignment of atomic planes from all crystals occurs in the friction contact. Micrograph used with permission from Reference 24.

atomic planes parallel to the surface after rubbing (22). The grains can also fracture and become loose particles that are extruded from the wear track, leaving a relatively thin (<200-nm), but well-adhered, (002)-oriented MoS_2 layer upon which counterface sliding occurs for the remainder of the coating's life (23) (**Figure 1*a***). Evidence of these deformation and/or fracture mechanisms has been reported in multiple studies of MoS_2-lubricated sliding contacts, with the dominant mechanism determined by the microstructure of the coating. For dense MoS_2 coatings that lack a columnar microstructure, reorientation occurs on the atomic scale, as demonstrated recently with in situ focused ion beam (FIB) and high-resolution transmission electron microscopy (HRTEM) techniques, allowing cross-sectional examination of an intact wear counterpart and coating surface (**Figure 1*b***). The direct HRTEM imaging of the sliding contact demonstrated that reorientation of several atomic layers at the interface accommodated sliding motion of the counterface (24).

Typical friction coefficients for sputtered MoS_2 films in vacuum or other inert environments are 0.005–0.05 (10, 25), with wear rates on the order of 10^{-8} mm^3 N^{-1} m^{-1} (10) for many counterface materials, again suggesting an average of ≈1 atomic layer of material removed for every ten 5-cm-long passes on the surface. In humid air, the friction coefficient of MoS_2 is generally 0.15–0.30, and the wear rate is one to three orders of magnitude higher than in vacuum, depending on the morphology (i.e., relative density) and crystallographic orientation of the film. The basal plane surfaces (002) are chemically inert, with a surface energy of approximately 2250 mJ m^{-2} (21), and are therefore less susceptible to water adsorption and oxidation than are the (100) plane edges (26, 27). Nevertheless, even highly (002) textured MoS_2 films lose 10–100 atomic layers per pass in humid air owing to oxidation, which increases adhesive wear, reduces cohesive strength (within the film bulk), creates blisters, and produces debris. The oxidized debris tends to be pushed out of the track rather than adhering to the counterpart and shearing (10), inhibiting the primary operative lubrication mechanisms discussed above.

Influence of doping on microstructure and properties. Because of the sensitivity to humid air, space components that require extensive testing or storage periods on Earth are sometimes lubricated with something other than pure MoS_2 to counteract degradation in the ambient environment, even if performance of the component will be less than ideal in its ultimate application (28). Improving the tribological performance of sputtered MoS_2 in humid air has been an active area of study for the past 30 years (29), with the aim of turning the material into a lubricant that can provide approximately the same low friction coefficient on Earth for thousands of operating cycles (i.e., testing) and in space for 1–100 million cycles over 15–30 years (as in a solar array joint, for example). On the basis of the degradation mechanisms described in the previous section, most

efforts to increase the wear life of sputtered MoS_2 in humid air have focused on the alteration of MoS_2 surfaces for reduced water and oxygen adsorption via film densification and neutralization of potential adsorption sites (28). Stupp (29) was the first to show that codepositing <10 atomic percent of different metals with MoS_2 resulted in a reduction of friction and wear of the sputtered coatings in air. Stupp attributed the performance enhancement to increased film density and hardness, especially with Ni additions. In this case, the metal dopant was distributed homogeneously throughout the coating material. Many studies followed on reducing the susceptibility of MoS_2 films to moisture with different dopants, including Pb (30), Au (23), and polytetrafluoroethlene (PTFE) (31). Most of these dopants also improved the lubricity of MoS_2 and other TMD materials (e.g., WS_2, $NbSe_2$, and $MoTe_2$) by increasing the interlamellar spacing and weakening the van der Waals interactions to further promote easy shearing (17). Carbon additions to burnished and bonded MoS_2 also improved MoS_2 performance in humid air. Among other beneficial functions, metal and carbon additives acted as oxygen diffusion barriers at edge planes and as oxygen scavengers in worn areas to reduce MoS_2 oxidation (19). Zabinski et al. (32, 33) later performed detailed studies of a well-known performance-enhancing additive, antimony trioxide, which was found to promote a microstructural rather than a chemical effect on MoS_2 lubrication, for which rubbing induced organization in the near surface of the material, where very thin (10-nm) layers of basal plane–oriented MoS_2 material on harder Sb_2O_3 surfaces evolved. In this layered architecture, the Sb_2O_3 provided wear and oxidation protection of the underlying lubricant material, which decreased the wear rate of the composite coating in humid air by two to three orders of magnitude compared to pure MoS_2. Structural analogs to those proposed by Zabinski et al. have since been fabricated by depositing MoS_2/Sb_2O_3 multilayers and also by depositing MoS_2-based solid lubricants on hard surfaces, patterned by laser etching and other methods to retain embedded volumes of MoS_2-based solid lubricants (34). These materials consistently demonstrate lower friction and wear rates than does MoS_2 alone, as did their original precursors.

Stiction: high static friction at interfaces

In a recent study of friction as a function of contact temperature from −80 to 180°C, a series of proven doped MoS_2 coatings was compared by measuring their steady-state wear rates with precise (±1-nm), in situ recording of wear track depth with white-light interferometry between passes of the counterface (**Figure 2**) (35). These measurements were previously very difficult to obtain because the low wear rates result in very small changes in contact surface topography, even after thousands of cycles. In this unique study, antimony trioxide–doped MoS_2 coatings demonstrated the lowest steady-state friction coefficient (0.03) and wear rate (10^{-8} mm^3 N^{-1} m^{-1}). Because atomically thin layers of intrinsic solid lubricants can endure multiple sliding cycles, atomic layer deposition (ALD) processes for lubrication of micro- and nanoscale electromechanical systems (MEMS and NEMS, respectively) with 5–20-nm-thick films of intrinsic lubricant materials are being examined to eliminate stiction problems at contact interfaces that currently limit the utility of these mechanical devices (36).

Influence of crystallographic structure on properties. The initial ≈50 nm of sputtered MoS_2 typically grows with basal planes parallel to the substrate (002 texture). Thus, for very thin (<50-nm) layers, the parallel orientation of MoS_2 basal planes is maintained. Controlled growth of humidity-resistant, (002)-oriented MoS_2 as found in very thin films can be sustained throughout the thickness of a 1-μm-thick coating by alternating its growth with very thin (<10-nm) metallic layers for improved resistance to humidity; films with predominantly (002) crystal line orientation are less reactive with the ambient environment (26, 27, 37). Researchers have investigated alternative approaches for protecting the reactive atomic edge sites of the MoS_2 crystal, including the use of dopants with large atomic radii, which are expected to substitute for Mo and S and induce curvature of the atomic planes (38), and the use of fullerene-like MoS_2 nanoparticle films (39).

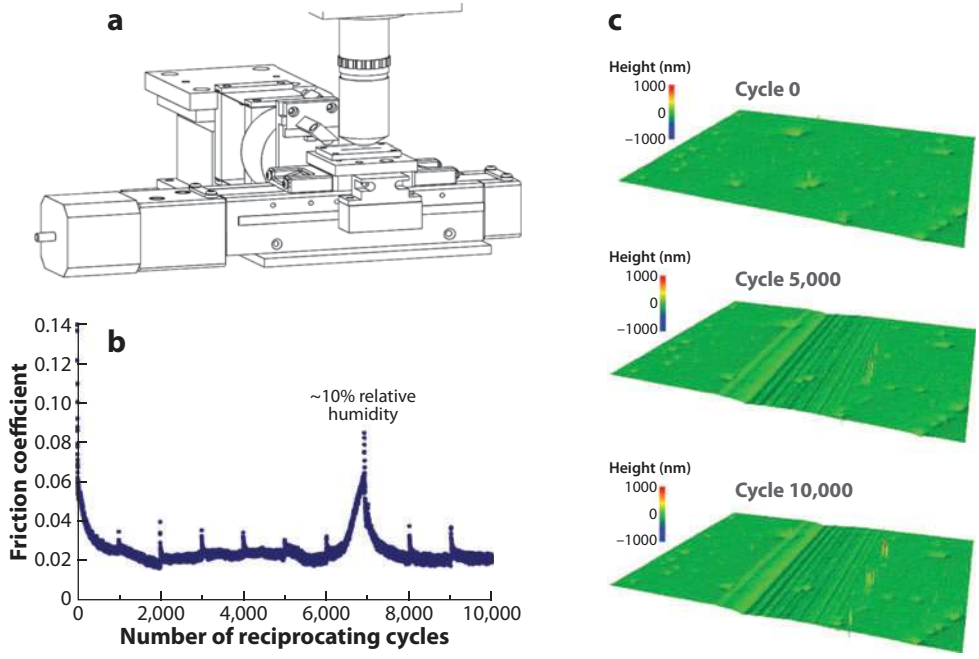

Figure 2

(*a*) An apparatus for measuring in situ wear rates. An Sb_2O_3-doped MoS_2 coating sample undergoes reciprocating sliding and is then relocated under a white-light interferometer with submicrometer precision so the wear rate in a selected region can be measured after a desired number of sliding cycles. (*b*) The friction coefficient is measured during sliding tests. Note the sensitivity of the friction coefficient on humidity as it rises upon the introduction of slightly humid air. (*c*) The series of 3-D topography scans was produced by the interferometer during the same test at the indicated number of cycles and demonstrates a relatively high wear rate of the coating material over the first 5000 cycles, followed by a very low steady-state wear rate. Unpublished images used with permission of the authors of Reference 35.

These novel approaches have yet to be rigorously tested, but initial results are promising. For example, MoS_2 films doped with W and Se endured more than 100,000 cycles in 40% humidity. The fullerene nanoparticles were reported to demonstrate vacuum-like performance in air, with a friction coefficient of <0.01 and a wear rate on the order of 10^{-8} mm^3 N^{-1} m^{-1}.

Progress toward atomic-scale structure control of intrinsic solid lubricants like MoS_2 and an improved understanding of their wear mechanisms are encouraging steps toward improved lubrication for space applications requiring long-term storage and preflight tests in terrestrial environments. Nevertheless, the current orders-of-magnitude differences in friction coefficients and in steady-state wear rates measured in air and in space (for ordinary hexagonal MoS_2) are too large for their use in components designed for extended or cycled operation in both environments.

Extrinsic Solid Lubricants

Like MoS_2, graphitic carbon has a structure that consists of covalently bound atomic lamellae, with weaker interplane bonding. Because of its layered structure, discovered by Bragg (40) with X-ray diffraction, graphite was thought to be an intrinsic lubricant until advances in aircraft technology allowed flight in a range of altitudes at which the concentration of water vapor was low, and graphite commutator brushes were found to wear at much higher rates than previously observed

(41). The laboratory work of Holm (42) and later Savage (43) in the 1940s revealed that the absence of condensable vapors, including water vapor, compromised the lubricity of graphite. In the case of graphite, the 66 kJ mol^{-1} binding energy between basal planes (44) would render the material intrinsically abrasive, with high friction and wear rates (45). The prevailing hypothesis of graphite lubrication has been based on weakening of interplanar bond strength by intercalation of water and similar polar molecules (e.g., alcohols, ethers, etc.) (46). The bond strength may be further weakened by the insertion of atoms or molecules between planes (47), as described for doped MoS_2. Recent X-ray diffraction studies of graphite surfaces with a synchrotron source (48), however, have shown that no difference between the near-surface basal plane separation of graphite in humid air and either that of the bulk or that of degassed surfaces in vacuum. This finding lends support to an alternative explanation of graphite lubrication, in which dangling σ bonds at edge planes that are initially present or generated during wear events are continually terminated by chemisorbed vapor molecules (49) to eliminate high-energy surfaces that would otherwise promote adhesive wear (50).

Diamond-like carbon (DLC): refers to a broad range of amorphous carbon films with different fractions of sp^2 and sp^3 bonds

Changes in local graphite bond configurations give rise to carbon allotropes with wildly diverse properties such as diamond, fullerenes, nanotubes, graphene, diamond-like carbon (DLC), and many others. These carbon structures all push the limits of useful materials properties for tribological applications, such as thermal conductivity [diamond (51), graphene (52), and nanotubes (53)], mechanical elasticity [fullerenes (54) and nanotubes (55)], and strength [DLC (56) and, of course, nanotubes (57)]. Similarly, there are various effects of the environment on these carbon-based materials. For this reason, and because of the potential held by carbon as a lubricant with broad applications, environmental effects on all the forms of carbon listed above have been the subject of many tribological studies. Here, only graphite and DLC coatings are reviewed because they are the most frequently occurring solid-lubricant films, but the reader is referred to macro- through nanoscale tribological studies and reviews of particular interest to the authors on nanotubes (58), fullerenes (59), and diamond (60–62) coatings.

Although some tribological principles observed on one size scale apply universally, some principles of carbon-based lubrication are strictly limited to the characteristic length scale on which they were determined. For example, Hirano and coworkers (63, 64) introduced the concept of superlubricity, which was recently examined further by Dienwiebel et al. (65). Both groups observed that the frictional force was reduced by orders of magnitude on a nanoscopic graphite-graphite interface when the lattice misfit angle in the contact was 45° owing to elimination of stick slip over individual atoms (66). The phenomenon, however, was limited to the nanoscale [possibly the microscale for mica (64)]. Recently, the hypothesized transfer of graphite to the W AFM tip to induce superlubricity at those initially heterogeneous interfaces as proposed by Dienwiebel et al. (65) was confirmed by Merkle & Marks (67), who performed nanoscale contact experiments inside a transmission electron microscope (TEM) on a very thin, electron-transparent polycrystalline graphite surface. Flakes of graphite wore away rapidly in the vacuum environment and adhered to a W tip whose proportions were similar to those of the tip used by Dienwiebel et al. (65). Researchers conducting macroscale tribology experiments should not expect to observe superlubricity originating from the sliding of incommensurate surfaces; however, they may see the phenomena manifested by a different mechanism for superhydrogenated DLC films, as is discussed below.

Diamond-like carbon. DLC films—thin amorphous carbon materials with a broad range of atomic structures and compositions (some DLC films are hydrogenated) that are tailorable with processing parameters—have been studied the most extensively of any of the carbon-based tribological coating materials. Within the family of DLC materials, there are several varieties.

Tetragonal-amorphous carbon (*ta*-C) refers to a subset of DLC materials with >40% sp^3 carbon hybridization (diamond bonding), mixed with sp^2 (graphite bonding) (68). Hydrogen may terminate carbon bonds in the random covalent network of carbon atoms that form DLC coatings and may prevent the formation of stable graphite during film growth (69). DLC is generally hydrogenated when it is deposited via ion beam or plasma-assisted chemical vapor deposition (CVD) techniques with methane, acetylene, or other hydrocarbon precursor gases. Alternative physical vapor deposition (PVD) methods use graphite as a precursor, offering the capability of hydrogen-free DLC growth. To obtain a high fraction of carbon in the sp^3 bonding configuration, local (atomic-scale) spikes of pressure and temperature must also occur at the surface during film growth. This is typically achieved by ensuring that depositing carbon species possess an average kinetic energy on the order of 50 to 150 eV. Lower incident ion energies are insufficient for the production of the required pressure-temperature spikes on the condensation surface, whereas higher-energy ions will create sp^3 network defects or may result in annealing of the surface into the stable sp^2 network (70, 71). The kinetic energy of incident species is higher than that typically associated with magnetron sputtering (1–5 eV) or CVD (0.5–1 eV), and thus DLC film processing requires a source of additional energy input (72).

Because many materials qualify as DLC, tribological results for these coatings demonstrate a large spread, with claims of friction coefficients as low as 0.001 and wear rates lower than 10^{-11} mm^3 N^{-1} m^{-1}. In humid air, the friction coefficient is generally 0.1–0.3, with a span of wear rates from 10^{-8} to 10^{-6} mm^3 N^{-1} m^{-1}, the variability of which is related to a hardness dependency on hydrogen concentration. Because most DLC coatings rely on the formation of graphitic, or graphite-like, wear debris and transfer films under typical contact pressures (73), the performance of these coatings is sensitive to the presence of water vapor, but these coatings do not necessarily have the same dependence on water vapor as does graphite, in which water vapor consistently reduces friction. Although there are outliers, DLC films follow a general trend in terms of the friction coefficients and wear rates observed under particular conditions, as well as the mechanisms underlying the performance of the coating materials. Hydrogen-free DLC materials demonstrate lower friction and wear in the presence of water vapor, as does graphite, with the same proposed mechanisms of intercalation for reduction of shear strength and/or termination of adhesive dangling bonds. Friction is reduced as the shear process induces bonding relaxation from a metastable sp^3 configuration to a sp^2 configuration that produces low-shear-strength transfer films (associated with a period of significant wear)—a process often referred to as contact surface graphitization (74–76). This mechanism occurs during the run-in period observed for many DLC materials, when the friction is initially high, but is reduced as graphitization and transfer film formation generally occur over hundreds to thousands of cycles. Hydrogenated DLC films, however, perform well in ultrahigh vacuum and other inert environments (77, 78), so long as some fraction of the self-contained supply of hydrogen distributed throughout the coating is present in the near-surface region (79, 80). Performance of a:CH films often degrades in the presence of humidity or other vapors, owing to surface coverage with oxygen or hydroxyl ions, resulting in increased adhesive forces in the friction contact (73). The presence of hydrogen in DLC has multiple impacts on the transfer film formation process. For relatively small contact loads and speeds in vacuum applications, hydrogen terminates dangling carbon bonds, which reduces friction and adhesive wear as the surface is passivated, resulting in interfacial shear, rather than intrafilm shear (81), as is typical for chemically inert, hard coating materials (8). This lack of adhesion to the sliding counterface also inhibits graphitic transfer film formation, which is attractive for MEMS and NEMS applications, for which debris associated with the transfer film formation process is detrimental for device performance. For loads and speeds corresponding to typical bearing and gear contacts, relatively soft hydrogenated DLC is prone to deformation by

plowing and abrasive wear. At higher contact loads and sliding speeds, frictional heating leads to the local release of hydrogen. This reduces the shear strength of the DLC materials and facilitates sp^3-to-sp^2 bond rearrangements in the contact area, resulting in graphitic transfer film formation (75).

One noteworthy variant of DLC is superhydrogenated, near-frictionless carbon (NFC), developed at Argonne Laboratories. In the NFC coating, a hydrogen-rich mix of gases is used to process the films, promoting termination of unsatisfied carbon bonds on the coating surface with one or perhaps more hydrogen atoms (82). [Molecular hydrogen termination was a long-held hypothesis. However, recent studies suggest that only atomic hydrogen coverage of NFC surfaces is present (83).] Erdemir et al. (82) believe that the hydrogen atoms lose their electron to the outer shell of the carbon atoms, leaving the positively charged hydrogen nucleus exposed. Thus, when two opposing surfaces are self-mated (both coated with NFC) and come in contact, the hydrogen-terminated surfaces electrostatically repel one another (11). The presence of humid air or other reactive ambient environments disrupts hydrogen termination of the sliding contacts, and friction increases with the concentration of reactive gas (84). Thus, an inert environment is required for observation of this unique tribological response. Friction coefficients measured during laboratory tests of NFC in nitrogen at an atmospheric pressure are on the order of 0.001, which is less than the resolution of the most tribometers—hence the NFC moniker. The wear rates are reported to be as low as 10^{-11} mm^3 N^{-1} m^{-1} for these materials under specific test conditions (11).

Near-frictionless carbon (NFC): diamond-like carbon deposited in an abundance of hydrogen and characterized by very low friction coefficients in inert environments

High-Temperature Lubricants

MoS_2 and carbon-based materials are both excellent lubricants with low wear rates and low friction coefficients—provided the ambient atmosphere is just right. Both materials not only are sensitive to ambient vapors (or the lack thereof) but have a limited range of operating temperatures. MoS_2 surfaces are rapidly converted at 350°C to molybdenum trioxide (85; C. Muratore, J.E. Bultman, A.J. Safriet & A.A. Voevodin, unpublished data), which is abrasive at temperatures of <500°C. Graphite, DLC, and most other carbon-based films oxidize in air at slightly higher temperatures (≈400°C) (85), resulting in increased friction and accelerated wear. Clearly, for lubrication at elevated temperatures, a different body of materials must be considered. Unfortunately, most materials that shear easily at higher temperatures are abrasive under the conditions in which MoS_2 or DLC is unparalleled as a solid lubricant. A brief summary of three approaches to high-temperature lubrication follows.

Noble metals. Ag and Au have a low shear stress with very limited sensitivity of mechanical properties to ambient vapor and temperatures (up to approximately half their respective melting points). As thin films on hard substrates, these soft metals serve as effective lubricants in X-ray tubes and satellite applications (4), which are typically in operation for years in high vacuum and occasionally at high temperatures—all conditions that preclude the use of liquid lubricants. Bowden & Tabor (7) investigated the principles of low-shear, pure-metal films on hard surfaces and determined that the interfacial shear strength was dictated by the soft film, whereas the maximum supported normal load was determined by the hard substrate. Thus, the friction coefficient (μ is the shear stress of surface/applied load) is much lower for this somewhat ideal bilayer system (7). The role of each layer became apparent in studies by Arnell & Soliman (86) and later by Spalvins (18), who examined the effect of soft metal layer thickness on the friction coefficient. In both works, a critical thickness in the range of 300 to 1000 nm (depending on the substrate roughness) yielding the lowest friction coefficients was identified. For thinner films, the friction coefficient was higher because full surface coverage of the metal was not obtained in the wear track. For thicker films, the

presence of the hard substrate was obscured, and a larger share of the load capacity was carried by the soft metallic film, resulting in the addition of a significant plowing force to the total tangential force (87). Arnell & Soliman (86) measured room-temperature friction coefficients between 0.2 and 0.4 for coatings close to the critical thickness.

Magneli phases: a homologous series of substoichiometric transition-metal oxides with slip planes that result in a reduced shear strength

Double oxides: bimetal oxide compounds such as Ag_2MoO_4 that often show low friction at moderate to high temperatures

Metal oxides. In addition to low shear strength in the desired temperature range, microstructural and compositional stability is also required of a candidate high-temperature lubricant. Many oxides demonstrate adequate stability up to 1000°C and above but are characterized by strong covalent bonding, which suggests that the surfaces would be difficult to shear. In fact, ceramic materials typically yield high friction coefficients (0.8 to 1.0) that generate high tensile stresses and produce surface cracks and debris particles (7). Magneli (88), however, discovered that substoichiometric oxides of several transition metals form a homologous series of compounds of the formula Me_nO_{2n-1}, Me_nO_{3n-1}, or Me_nO_{3n-2} with planar lattice faults that result in crystallographic shear planes with reduced binding strength. A few years after Magneli's results were reported, Peterson et al. (90, 91) studied the potential of several oxide compounds as high-temperature lubricants in powder form. In Peterson et al.'s work, MoO_3 and other oxides demonstrated a friction coefficient of 0.2 at 700°C. In fact, several transition-metal oxides (e.g., WO_x, VO_x, etc.) were shown to deform by plastic flow at high temperature rather than by brittle fracture at elevated temperatures. Three decades later, Gardos et al. (89) extensively studied the rutile allotrope of titania as a high-temperature lubricant and correlated Magneli's concepts with tribological phenomena. These researchers built a device to alter anion vacancy concentrations (by heating) to show that oxygen vacancy formation influenced the shear stress of rutile and to determine the lower limit on that shear stress for the material (89). Gardos et al. found friction coefficients ranging from 0.15 to 1.5 and wear rates between 10^{-6} and 10^{-4} mm^3 N^{-1} m^{-1}; both these variables had a strong dependency on the ambient atmosphere (air or argon). Generally, the friction coefficients for single transition-metal oxides forming Magneli phases range from 0.2 to 0.5 at homologous temperatures >0.7 (90), in agreement with Gardos et al.'s data.

Peterson et al.'s (91) work from the 1950s also included investigations of double oxides—molybdates and tungstates in particular. Some of these materials stood out for remarkably low friction and wear at 700°C—in fact, they were notable enough to be revisited 50 years later, as is discussed below. Although Peterson et al.'s results were often published in reports to government agencies that may be difficult to obtain, Erdemir (92) recently summarized many of his results as he examined the relationship between ionic potential of metal oxides and, for double oxides (e.g., PbO-MoO), the difference in relative ionic potentials of the oxides and their shear strength.

Formation of low-shear crystal planes is not the only mechanism by which oxides can provide lubrication. Oxidation of some metals results in a reduction of the melting point, thereby forming a lubricious glaze with low shear strength at high homologous surface temperatures.

Alkaline halides. During the development of early supersonic aircraft such as the RS70, which was reported to incorporate solid lubricants in 1000 applications with anticipated exposure to air at 800°C, researchers at NASA pioneered the use of fused alkaline halide eutectic coatings. Sliney et al. (9) studied CaF extensively because of its predicted stability in both air and liquid sodium, which was used as a coolant for the bearing application of interest at the time. These adherent coatings formed low-shear-strength surfaces, or glazes, at very high temperatures (500–900°C), close to their melting points, with friction coefficients of approximately 0.2 and low wear rates (which unfortunately were reported in nonstandard units). At temperatures of <500°C, thin-film materials like CaF and CeF improve wear resistance but have friction coefficients of <0.3 (85, 93)

and have been reported to be especially brittle at low temperature after one thermal cycle in air (94), suggesting strong environmental sensitivity.

DEVELOPMENTS LEADING TO ADAPTIVE COATING MICROSTRUCTURES

From the work reviewed above, it is apparent that selecting a solid lubricant that will perform in a narrow range of temperatures, gaseous environments, and other ambient conditions is straightforward. If an application will operate exclusively in vacuum or another inert environment, an intrinsic lubricant (e.g., a lubricious TMD) is an obvious choice because it will last millions of cycles under high loads. In ambient terrestrial conditions in which water vapor is abundant, a carbon-based solid lubricant would be suitable, providing low wear rates and very low friction. But what does one use on a deployable satellite structure subjected to thousands of sliding test cycles on Earth and then millions of operational cycles in space—or, even more challenging, on a reusable air-space vehicle capable of multiple atmospheric reentries and designed to have a maintenance schedule comparable to that of an ordinary aircraft? Some researchers maintain hope that a single-phase coating material that can provide low friction through a broad range of ambient humidity and temperatures for a useful number of cycles will emerge, but a more promising path of incorporating multiple lubricants in a composite coating material has been investigated and is the basis for the adaptive coating materials reviewed below.

Early Composite Solid-Lubricant Materials

Until recently, the best examples of a composite material designed to provide low friction over a span of temperatures from 25°C to 800°C in air or vacuum were the PS series of thick (250-μm) plasma-sprayed coatings developed at NASA by Sliney (87, 95) and DellaCorte (96), with alkaline fluoride compounds and noble metals mixed with hard phases, such as nickel chromium (PS 100) (95), chromium carbides (PS 200) (87), or oxides (PS 300) (96), for load support and reduced abrasive wear of the soft lubricant materials. Ag was selected as a low-to-moderate-temperature lubricant phase, and alkali fluorides were selected for high temperature in all PS coatings. These materials demonstrated friction coefficients between 0.2 and 0.6 over the target temperature range, depending on temperature, counterface material, and wear test method (e.g., oscillating journal bearing or pin-on-disc). Under certain conditions, friction coefficients of 0.2 to 0.3 from 25°C to 850°C were measured for all PS 200 and PS 300 lubricants. However, owing to the plasma spray deposition method, the coatings had a rough, coarse-grained surface appropriate for some applications, but not for precision components for which tolerances required smooth surfaces (18). Furthermore, the coarse grains (50–250 μm) resulted in excessive vibration during pin-on-disc wear tests, especially at lower sliding speeds, because the inhomogeneous surface consisted of lubricant phases separated by hard phases over long distances compared with the size of the friction contact; therefore, complete coverage of hard surfaces with lubricant was never attained (95). Sliney et al. (97) and others (98) did investigate smoother, fine-grained sputtered varieties of PS coatings, which demonstrated higher friction coefficients and wear rates compared with their plasma-sprayed counterparts. The most recent PS 300 generation of these coatings provides friction coefficients from 0.2 to 0.6 (depending on counterface and temperature) and moderate wear through a temperature range of 25–1000°C (96). The coatings are machinable and have improved stability at high temperature compared with the PS 200 and PS 300 series but still possess a rough texture. Although the PS coatings have some shortcomings, they were the first materials of their kind and demonstrated an important principle used in the current state of the

art, as stated explicitly by Sliney (95): Different phases of fresh lubricant could be incorporated within a hard composite matrix, to be exposed by the wear process as needed.

Nanocomposite Thin Films

The development of chameleon coatings was also influenced by the strong focus and rapid development of high-strength nanocomposite materials that were often composed of a combination of relatively low-strength phases. Early works revealed that a reduction in length scale of layer thicknesses or grain sizes in solid films could be used to control dislocation formation and that elastic modulus mismatch between components in layered or homogeneous composites could be used to inhibit dislocation mobility (99–101). Initial demonstration of these principles in coating materials sparked a period of intensive research in nanolaminate coatings (102–104). For increased hardness, the required materials possess sharp, strained interfaces and periodicity in the 5–10-nm range (105, 106). These architectures, sometimes referred to as superlattices (107), demonstrated high hardness but were very sensitive to variations in periodicity and were therefore difficult to deposit, especially on surfaces with significant topographic variation (e.g., a cutting tool). These findings motivated research on homogeneous hard nanocomposites, which were developed by Veprek (108), Veprek & Reiprich (109), and later by others, with crystals of 3–20 nm or less in an amorphous matrix. Many different elements have been incorporated into films with a nanocrystalline-amorphous structure, increasing hardness values up to 100 GPa for ceramic matrix composites (110, 111), and a maximum of 30–40 GPa for hydrogen-free DLC matrices (112, 113).

Although there is a relationship between strength and hardness, resistance to fracture also plays a significant role in tribological coatings when high contact loads are encountered. This combination of hardness and ductility necessary to produce a tough material is, of course, a classical challenge in the field of materials science, although nanocomposite coatings provide a promising answer to this challenge, with high hardness and a large relative volume of grain boundaries between crystalline and amorphous phases to deflect, split, and terminate growing cracks (114). To further improve ductility at the expense of superhardness, multilayer (115, 116) and graded (117, 118) composites can be produced. Alternatively, a more attractive option is the selection of a matrix phase with a lower elastic modulus in a homogeneous composite. Various tough nanocomposite TiC/DLC and WC/DLC coatings (both with a DLC matrix) (119), and materials with an amorphous YSZ-Au matrix (120), have shown high hardness ($\approx$20 GPa) and toughness.

Composites Employing Synergistic Lubricant-Lubricant Interactions

By incorporation of nanoscopic volumes of solid-lubricant materials in a hard matrix, the principle evidenced by the NASA's PS series of coatings, in which buried pockets of fresh lubricant could be exposed to replenish the friction contact with low-shear material throughout the wear process, could be coupled with the benefits of increased hardness and toughness observed for nanocomposite films. Donley & Zabinski (121) first proposed this approach and added that that the lubricant phases should be selected such that useful interactions with one another and with the ambient environment should occur over the anticipated operating conditions. This, they proposed, would both reduce friction and wear coefficients at room temperature and broaden the temperature range in which low friction was observed. Pure lubricant composites (with no hard matrix) were examined initially to identify useful interactions between compounds. PbO-MoS_2 was the first temperature-adaptive tribological coating material of this nature: Lubricant phases were selected

on the basis of anticipated improvements in room-temperature performance of MoS_2 with the PbO dopant, in addition to the formation of lubricant phases suitable for moderate and high temperatures upon heating, as predicted by a thermodynamic analysis of the Gibbs free energy of formation of possible compounds (122, 123). In this case, the $PbMoO_4$ and MoO_3 were formed on the coating surface after heating to 500°C. The results were consistent both with the works of Peterson et al. (91) discussed above, in which single-metal and bimetal lead oxides were among the best high-temperature lubricants, and with the findings of Magneli (88), who studied oxides such as MoO_3, which, when rich in atomic defects, possess low-shear planes. The coatings also outperformed pure MoS_2 under identical room-temperature conditions, showing the benefits of the composite material at high and low temperatures. Zabinski's work with multiple solid lubricants continued with other compounds, including WS_2-ZnO (both were lubricious at room temperature and formed $ZnWO_4$ and WO_3 at high temperature) (3, 124) and WS_2-CaF (which formed lubricious $CaSO_4$ at high temperature) (94), demonstrating a new family of coatings with multiple lubrication mechanisms over a broad temperature range in addition to room-temperature performance that was often superior to the performance of the single-lubricant compounds. Other researchers found that additional binary systems formed lubricious double oxides over the 25–800°C range of interest, including CuO-MoO_3 (125) and MoO_3-Ag_2O (126). All these coatings, however, demonstrated irreversible temperature adaptation in that after heating, their lubrication properties were lost at reduced temperatures owing to the presence of abrasive oxide compounds. Nevertheless, examination of this binary-compound approach to temperature-adaptive lubrication was another important step toward reversibly adaptive nanocomposite lubricant coatings.

CHAMELEON COATINGS

The concept of nanoengineering surfaces to provide multienvironmental tribological performance, with hardness and toughness to resist abrasion and fatigue wear in a heavily loaded contact by merging multiple complementary solid lubricants in a nanocomposite coating, created a basis for exploration of novel approaches to solid lubrication. With the nanocomposite concept in place, it was still necessary (*a*) to select coating compositions that would enable self-release of the appropriate stored lubricant material for each of the anticipated operational environments and (*b*) to provide a means to guide nanoscopic volumes of material to the contact zone for on-demand formation of macroscopic solid lubricating films. It was anticipated that coatings incorporating these design elements would provide a continuous response of the contact surface to the surroundings (load, sliding speed, environment, temperature) by self-adjusting to maintain the most favorable composition and structure in the sliding contact under the range of anticipated ambient conditions shown schematically in **Figure 3*a*** and ***b***. The concept is not too different from the natural defense mechanisms of chameleon lizards, whose surroundings automatically induce an alteration of skin to best evade predators. Thus, the term chameleon was used to describe early adaptive tribological nanocomposite coatings to highlight the features of self-regulating surface chemistry and microstructure to avoid coating failure (analogous to death by predatory friction and wear) in air-space transitions and in broad temperature ranges.

Air-Space Adaptation

Initial research on chameleon coatings was focused on adaptation to both extremes of terrestrial and space environments experienced by some aerospace components (e.g., deployable satellite structures) via two independent mechanisms. The coatings were produced with a hybrid process with two magnetron sputtering sources (one fitted with a WS_2 cathode and the other, pure W)

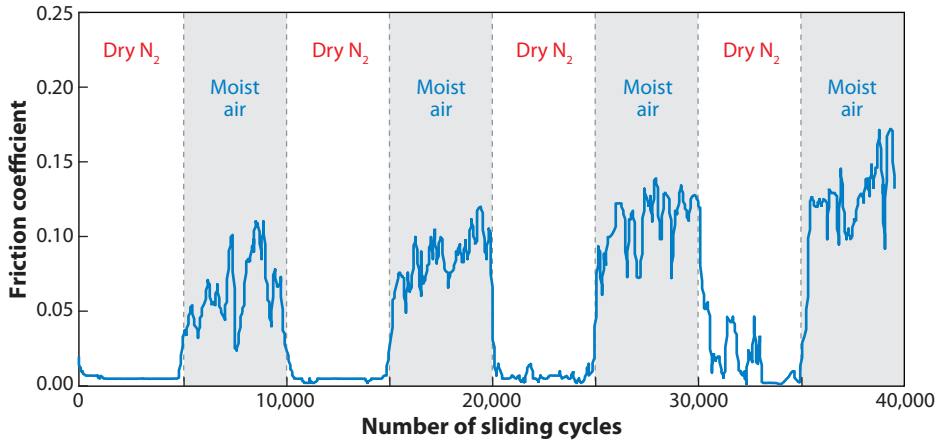

Figure 3

Friction measurements on a W-C-S coating surface over multiple exposures to dry and humid air. Plot from Reference 119 is used with permission from the publisher.

and a carbon pulsed laser deposition (PLD) target. The power to the WS_2 cathode was adjusted to control the sulfur content necessary to produce a nanocrystalline dichalcogenide phase as an intrinsic-lubricant phase for vacuum environments. The laser parameters were adjusted to provide carbon for the formation of WC and DLC phases assembled as shown in **Figure 3** to obtain a hard material also capable of lubricating in humid air (127, 128). Hardness was related to sulfur content, with a sharp drop from 17 GPa at sulfur contents below 20 atomic percent to approximately 7 GPa for higher sulfur contents. A W20-C60-S20 (in atomic percent) nanocomposite material yielded a friction coefficient comparable to that of pure graphite (0.15–0.2) in humid air and yielded the equivalent friction coefficient of pure WS_2 (>0.05) when the material was tested in vacuum. In vacuum, the 500-nm-thick coating provided low friction for $>2 \times 10^6$ cycles with a wear rate less than 10^{-7} mm^3 N^{-1} m^{-1}, demonstrating that the addition of a humidity-adaptive component (carbon) did not compromise the wear rate in vacuum but rather yielded an improvement when compared with monolithic WS_2 (129). When a continuous wear test was performed in a cycled environment of vacuum and 40% relative humidity, the friction coefficient reversed between the values expected for WS_2 and carbon alone for more than 40,000 cycles (**Figure 3**). This was the first demonstration of reversible adaptation to humidity in a single coating surface. Following the W-C-S chameleon coating example, other papers demonstrated a similar reversible adaptation to humidity in several other tough and hard nanocomposite coatings with similar architectures, including YSZ-Au-MoS_2-DLC (130, 131), and Al_2O_3-Au-MoS_2-DLC (132). These works illustrated the generality of the chameleon coating concept shown in **Figure 4** for many materials systems with a similar coating architecture, in addition to the concept of using hybrid PVD processes to insert multiple nanoscopic lubricant phases in a hard oxide matrix.

Mechanisms of air-space adaptation. Several research groups have proposed multiple mechanisms for the humidity-adaptive response of W-C-S and other nanocomposite coatings subjected to environmental cycling. The original authors (127, 128) investigated the adaptive mechanisms occurring in W-C-S coatings while in contact with a 440C steel ball and a contact stress of 0.6 GPa. From the friction coefficients under cycled vacuum–humid air environments, coupled with ex situ Raman spectroscopy analysis of the coating wear track, debris, and transfer film, it was

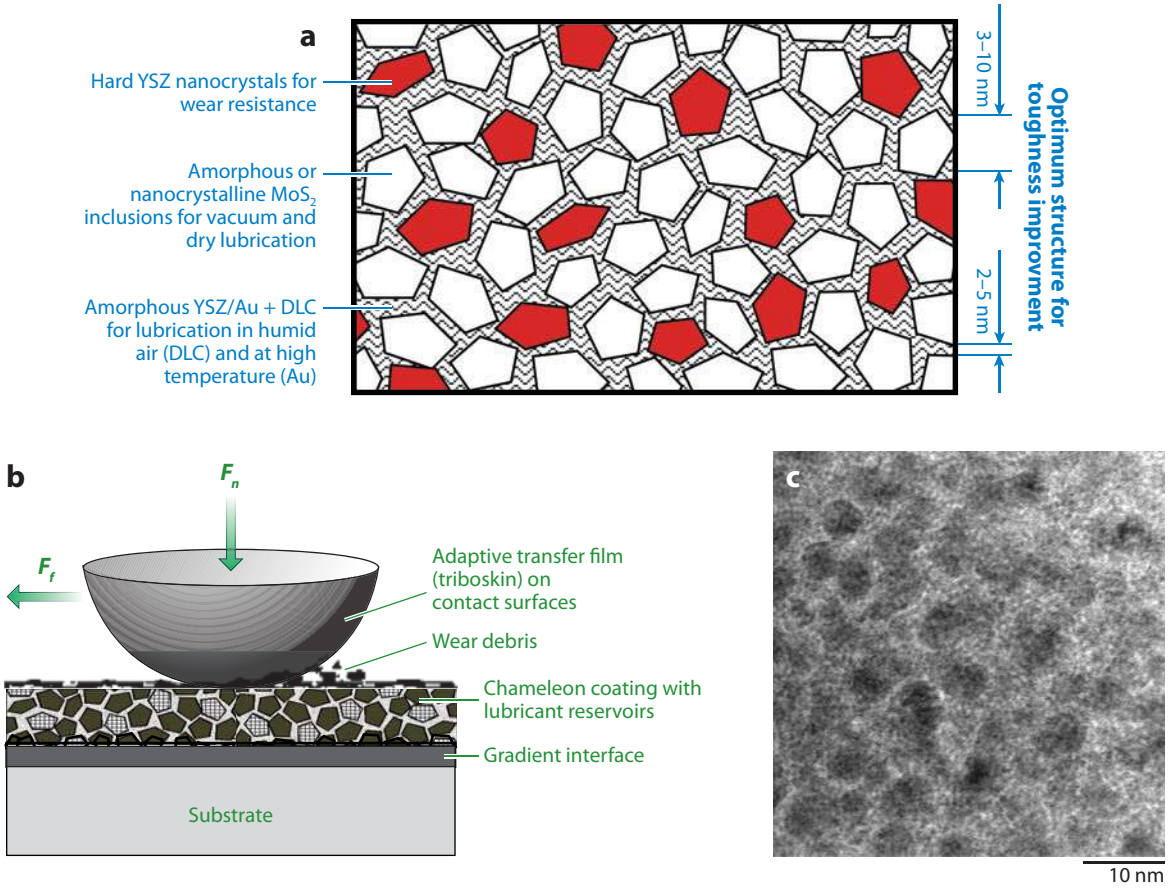

Figure 4

Schematic of a YSZ-MoS_2-DLC-Au coating: (*a*) microstructure and (*b*) response to sliding in different ambient environments. (*c*) A micrograph of the coating shows inclusions of MoS_2 in a nanocrystalline-amorphous YSZ-Au matrix. Adapted with permission from the publisher of Reference 130.

determined that carbon served as the active lubricant in humid air as the moisture-sensitive TMD became abrasive and induced a brief period of accelerated wear, exposing fresh carbon stored in the tungsten carbide matrix (127, 128). Intercalation and/or termination of graphitized carbon with water molecules resulted in a low-shear contact among potentially abrasive phases such as WO_3. Similarly, when the environment was altered from humid air to vacuum, the graphitic carbon at the surface of the friction contact wore away rapidly, and the nanoscopic volumes of TMD were exposed and collectively provided sufficient lubrication over the volume of the contact (one atomic layer of TMD was sufficient for multiple passes). In vacuum, the wear rate was lower for the nanocomposite than for monolithic WS_2 coatings of comparable thickness when tested in the environment for which they were best suited. This reduced wear rate was attributed to the presence of the hard DLC and WC phases within the nanocomposite architecture, as the applied load was distributed over this harder surface, reducing susceptibility of the soft lubricant to abrasive wear.

Rigney and colleagues (133, 134) performed similar tests on W-C-S chameleon coatings, but with half the initial value of contact stress (0.3 GPa) and a 440C cylindrical pin, and reported on

surface chemistry of the coating wear track and counterpart based on postmortem Raman and scanning electron microscopy (SEM) investigations. The coatings demonstrated similar adaptive performance in multienvironment testing. However, the phase composition of the transfer films in the wear track was not as distinct; no evidence of crystalline WS_2 or graphite was detected. This may have been due to the lower contact stresses (related to the graphitization of DLC discussed above).

Chromik et al. (1) performed reciprocating tests on a series of humid-dry adaptive YSZ-Au-MoS_2-DLC coatings at a higher contact stress of 0.9 GPa with optically transparent sapphire balls, which allowed in situ optical imaging of the coatings and the transfer film accumulated on the ball, in addition to determination of the thickness of the transfer film with ≈10-nm resolution via the appearance of optical interference fringes. This technique allowed correlation of transfer film characteristics to friction behaviors such as run-in periods, in which the transfer film increased in thickness to a steady-state value coincident with stabilization of the friction coefficient immediately or over several cycles, depending on film composition. In addition, occasional friction spikes (temporary increases in friction coefficient to values >50% of steady-state value) were observed. These events were correlated with sudden, localized removal of transfer film material adhered to the counterpart, which allowed return of the system to its steady state. In this work, ex situ Raman spectroscopy was used to examine contact surfaces. Both MoS_2 and graphitic carbon were detected in transfer films after testing in humid and dry environments. Preferential lubrication by one phase over the other can take place from a few monolayers on the surface, but such analysis would be beyond the detection limits of the Raman technique, which penetrates to depths on the order of 50–100 nm in materials such as DLC or WS_2 (30, 135). The recorded friction coefficients suggest that MoS_2 alone is not lubricating during high-humidity cycles; the observed values <0.1 are lower than are typically observed, even with the addition of dopants. There may be a synergistic relationship of graphite and MoS_2 in high humidity, whereby degradation of MoS_2 via multiple mechanisms (i.e., delaying mechanical interlocking of crystallites caused by, e.g., oxidation) may contribute to enhanced MoS_2 lubrication at room temperature (19). Although there is still an ongoing discussion of observed adaptive mechanisms and surface compositions among the groups performing the studies, differences may be attributed to test conditions (e.g., applied loads, counterface materials, wear test geometry). In situ microscopy experiments, with a focus on atomic layers at surfaces involved with sliding shear accommodation (as shown in **Figure 1*b***) under similar contact pressure and sliding speeds, are needed for a definitive discussion. Regardless of the exact mechanisms for adaptive surface changes under cycled environments, the materials demonstrated reversible adaptation to air and space conditions and superior performance in static environments, maintaining low friction and wear in all tests.

High-Temperature Adaptation

The nanocomposite chameleon concept was first demonstrated for humid-dry adaptation with several coating materials, but the challenge originally sought by Donley & Zabinski (121) was temperature adaptation. Within the chameleon coating architecture outlined for air-space adaptation, individual high-temperature lubricants could be added to expand the concept to lubrication over elevated temperatures and, ultimately, to multiple lubricants to achieve low friction surfaces over a broad range of temperatures.

Diffusion-based adaptation for moderate temperatures (<500°C). YSZ-Au-MoS_2-DLC was previously listed among the first air/space adaptive nanocomposite coatings. Au was added to this composite for two purposes—(*a*) as an intercalant or microstructural aid for reducing the

shear strength and improving the humidity resistance of MoS_2 and (*b*) for lubrication at elevated temperatures in air or vacuum. When this coating was heated to 500°C, nanoscopic grains of Au coalesced on the surface, providing a low-shear interface on a hard surface capable of supporting the applied load of the friction contact (130, 131) and thus, as discussed above, a reduced friction coefficient. Subsequent works focused on the binary YSZ-Au system indicated that up to 20 atomic percent of nanocrystalline Au could be introduced into the YSZ before significant softening (to values <15 GPa) occurred (120). Coatings with 10–20% Au had high ductility. These films provided friction coefficients of approximately 0.2–0.4 from room temperature to 500°C against sapphire (136), consistent with that observed for noble-metal films on hard substrates. One significant implication of this work was that soft nanocrystalline lubricant phases could be incorporated into a hard ceramic matrix and demonstrate thermally activated, collective behavior in a friction contact. Other studies of noble-metal nanocrystals imbedded in ceramic matrices followed, including TiC/Ag (137) and later YSZ-Ag (138) and CrN-Ag (139, 140). These initial studies of Ag-lubricated hard surfaces demonstrated friction coefficients between 0.2 and 0.4 for 10–20 atomic percent Ag in the same 25–500°C temperature range. The wear rate of such materials is difficult to quantify, because the thickness of the film changes (sometimes substantially) as the Ag coalesces to the surface, and is often not reported in these initial studies of temperature-adaptive coating materials.

Detailed descriptions of the driving forces behind noble-metal phase segregation and coalescence on the YSZ surface in YSZ-Ag with 15–30 atomic percent Ag can found in the literature (141, 142). To summarize, the coatings are produced in a metastable condition by forced codeposition of metal and crystalline YSZ at a substrate temperature of 150°C. As deposited, the noble-metal atoms are distributed as nanoinclusions throughout a matrix of nanocrystalline-amorphous YSZ, with a large interfacial energy. Heating activates diffusion of Ag out of the strained YSZ, in which diffusion is rapid throughout its highly defective structure. The driving force to reduce total system potential (due to strain) and surface energy (due to high initial YSZ-Ag interfacial energy) results in Ag migration from the subsurface to the surface. This creates a composition gradient within the coating to drive diffusion from the bottom of the coating to the top of the coating, resulting in rapid noble-metal coalescence at the surface, even when the coating is heated to moderate temperatures. In situ studies are presently being carried out to identify the additional role of thermal gradients on mass transport in these systems. Thermally activated segregation of noble metals to the surface results in a low-shear-strength interface with the friction contact that is not adversely affected by interactions with most ambient atmospheres, providing suitable lubrication up to 500°C.

Adaptive lubrication of surfaces by Au or Ag does have some shortcomings, including poor adhesion at elevated temperatures in the presence of oxygen (91) and excessive deformation at elevated temperatures in the contact (87). Additionally, when the lubricant segregates at high temperature, the strength and mechanical stability of the matrix can be compromised, as has been shown by higher wear rates in CrN-Ag (139) and recently in TiN-Ag (143) composites when these materials are tested at elevated temperatures. Finally, the supply of lubricant within the volume of the coating material is depleted rather quickly by metal diffusion to the coating surface upon heating—in the case of YSZ-Ag, the coating was depleted of Ag within 5 min of heating to 500°C.

Tribo-oxidative mechanisms for very high temperatures (>500°C). Perhaps the most common temperature-adaptive mechanism observed in the tribological coatings community is tribo-oxidation. For example, TiAlN and many other cutting tool coating materials are based on hard phases with metal additions that form thermally stable protective oxide layers (144). Such layers can be somewhat lubricous, with friction coefficients of 0.3–0.6 and low wear rates. Self-hardening

mechanisms in TiAlN coatings can occur over extended periods at high temperature owing to spinodal decomposition to further increase wear resistance (145). The properties of these thin-film compounds are sometimes modified further with one or more elements, such as vanadium (146), that are known to form Magneli phases at very high temperatures (>600°C), which, as discussed above, can demonstrate additional useful properties of oxidation stability, low adhesion, and easy shear. Recent studies have included exploration of Mo-N- and W-N-based coatings, designed to oxidize in dry machining operations in which very high contact temperatures are common, to create wear-resistant and somewhat lubricious oxide phases upon heating (147). This mechanism was also investigated in YSZ-Mo adaptive nanocomposite coatings. The addition of Mo resulted in hardening of the coating (by the mechanisms described in the Nanocomposite Thin Films section above) and reduced friction at 700°C from 0.8 for pure YSZ to 0.4 for low MoO_3 concentrations (138). Unfortunately, cracking at the coating surface due to rapid growth of subsurface MoO_3 crystals and some sublimation of the material were observed. Other metals such as W, expected to form oxides with a higher temperature threshold for sublimation, have been investigated in the YSZ matrix but did not yield the low friction coefficient observed for Mo from 500°C to 700°C (C. Muratore, J.E. Bultman, A.J. Safriet & A.A. Voevodin, unpublished data).

Broad-range temperature adaptation (25–700°C). To allow effective molybdenum oxide lubrication at very high temperatures, researchers examined YSZ-Ag-Mo composites, in which Ag could rapidly diffuse to the surface as a protective coating and a moderate-temperature lubricant (138). A further increase in temperature resulted in Ag extrusion from the wear track. The extrusion exposed a small volume of Mo to the oxidizing atmosphere for localized production of lubricious MoO_3 in the exposed contact area, thus eliminating destructive, homogeneous MoO_3 formation, previously shown to result in severe cracking (**Figure 5**). It was also expected that lubricious silver molybdate phases (126) would form to lubricate at mid-range temperatures (400–600°C). These YSZ-Ag-Mo coating materials were investigated over the 25–700°C temperature range and were the first chameleon coatings to demonstrate broad-temperature-range lubrication via two distinct temperature-adaptive mechanisms, resulting in a moderate friction coefficient of 0.4 throughout. Analysis of the coatings revealed that the contact surfaces were composed entirely of Ag from 25°C to 500°C and of MoO_3 at temperatures above 500°C. The formation of lubricious silver molybdate compounds, such as those examined by Gulbinski & Suszko (126), did not occur. This lack of reactivity between components may have been due in part to the lack of contact of the Ag and Mo because of rapid segregation of the Ag out of the matrix and to the surface. To facilitate silver molybdate compound formation and to decrease low-temperature friction, small fractions (<10 atomic percent) of MoS_2 were added during deposition of the coating (148). The MoS_2 was effective as both lubricant and catalyst; the friction coefficient dropped to below 0.2 from 25°C to 700°C for a series of coatings with different compositions, and double-metal-oxide formation was observed. The low friction coefficients observed were attributed to the presence of MoS_2 and Ag at <300°C, silver molybdate compounds from 300°C to 600°C, and MoO_3 at higher temperatures. Wear rates of these materials were moderate, but the friction coefficients were the lowest reported for any material over this temperature range, demonstrating how a coating incorporating all chameleon coating principles of nanoscopic, synergistic lubricant phases in a tough, inert matrix would provide a way forward for broad temperature lubrication. Recent works, including coatings consisting of a Mo_2N matrix with nanoscopic MoS_2 and Ag lubricant phases (149) and bulk composites (150), have followed. The crystallography of these somewhat complex bimetal oxide crystals is not always well understood. Aouadi and colleagues (151) have made a correlation to layered atomic structures developing at high temperature with weak Ag-O interlayer bonds as a possible explanation for the low friction coefficients in Ag-based double oxides.

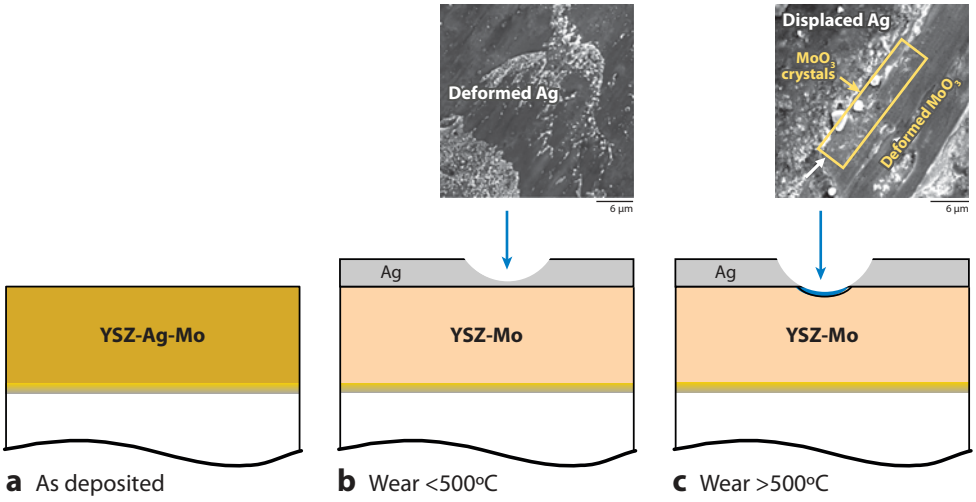

Figure 5

Multiple adaptive mechanisms at different temperatures for the YSZ-Ag-Mo coating material, in which Ag migrates to the surface to provide lubrication at <500°C and is pushed out of the wear track to expose Mo embedded within a YSZ matrix at higher temperatures. Schematic of coating wear at different temperatures is redrawn from Reference 138 with permission from the publisher.

Reversible Adaptation Over a Broad Temperature Range

The only remaining obstacle for true chameleon-like behavior in thermally adaptive tribological nanocomposites was reversibility of the contact surface over multiple thermal cycles, analogous to its humidity-adaptive counterpart. Just like the first temperature-adaptive thin-film lubricant material ($PbO\text{-}MoS_2$), the most recent ($YSZ\text{-}Ag\text{-}Mo\text{-}MoS_2$) was abrasive after heating. For adaptation reversibility over temperature cycles, some lubricant must be preserved in the as-deposited state. As temperature adaptation took place primarily via two mechanisms—diffusion of noble metals to the surface and oxidation of components within the coating—architectures incorporating lubricant and oxygen diffusion barrier layers were explored. It was postulated that a microlaminate coating with alternating adaptive coating layers and diffusion barrier layers would inhibit Ag or Au diffusion out of underlying layers and would allow the noble metal to remain homogeneously distributed throughout the matrix as the energetically desirable free surface was no longer present (until breached by the wear process). The diffusion barrier layers would also restrict oxygen diffusion into the coating to avoid molybdenum oxide formation until needed. Both Ag diffusion and transition-metal oxide formation would occur on demand in such a material, in which the coating immediately below the next intact diffusion barrier layer would essentially be in the as-deposited condition and be ready to adapt to any ambient temperature upon exposure by the wear process, just as a monolithic adaptive coating would.

Researchers produced test architectures to examine the concept, including deposition of a two-layer coating with a patterned diffusion barrier atop a YSZ-Ag-Mo lubricant layer (142). The diffusion barrier was patterned with holes of a diameter consistent with the characteristic length of a shallow wear track to simulate exposure of a fresh lubricant layer. **Figure 6** shows that Ag flow did occur laterally through the diffusion barrier mask, resulting in modulated lubricant supply that extended the coating life by more than a factor of 10 (the wear rate was much less than 10^{-6} mm^3 N^{-1} m^{-1}) compared with a single YSZ-Ag-Mo lubricant layer of the same thickness.

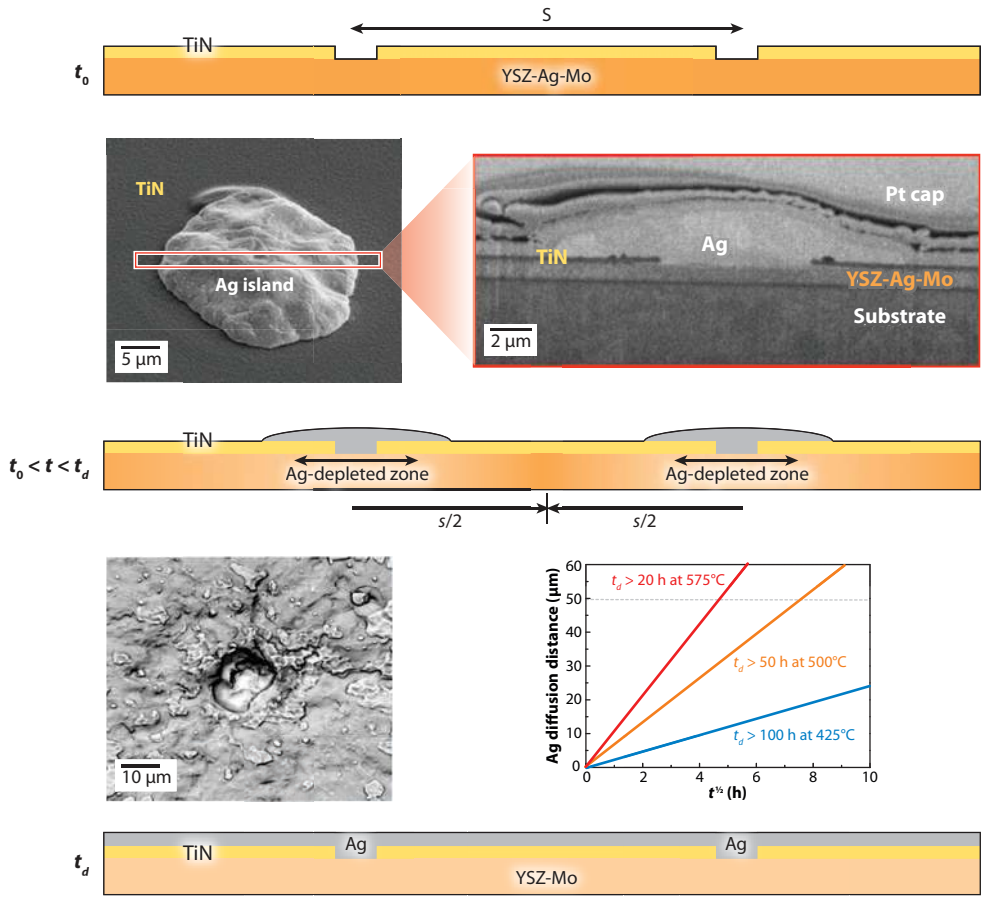

Figure 6

A homogeneous, temperature-adaptive coating layer with a diffusion barrier mask patterned with holes a distance of s apart is heated starting at t_0. Ag migrates from the adaptive coating layer to the surface of the diffusion barrier only through its holes ($t_0 < t < t_d$), until the Ag is depleted at $t = t_d$. On the basis of calculations of the diffusion coefficient of Ag in the YSZ-Mo matrix, the time for lubricant depletion at a constant temperature can be predicted. The time to depletion can be adjusted by manipulating the number of holes in the diffusion barrier mask. Micrographs from Reference 142 are used with permission from the publisher.

This architecture also provided insight with respect to the nature of diffusion in the YSZ matrix and allowed simple estimation of the lifetime of the lubricant supply within the adaptive lubricant layer and its dependency on the density of holes on the surface and on ambient temperature.

A multilayered coating with two adaptive lubricant layers and a diffusion barrier between them was then examined. Just as a monolithic coating, the topmost adaptive coating layer fails to attain true chameleon or adaptive status as it was limited to one irreversible change. However,

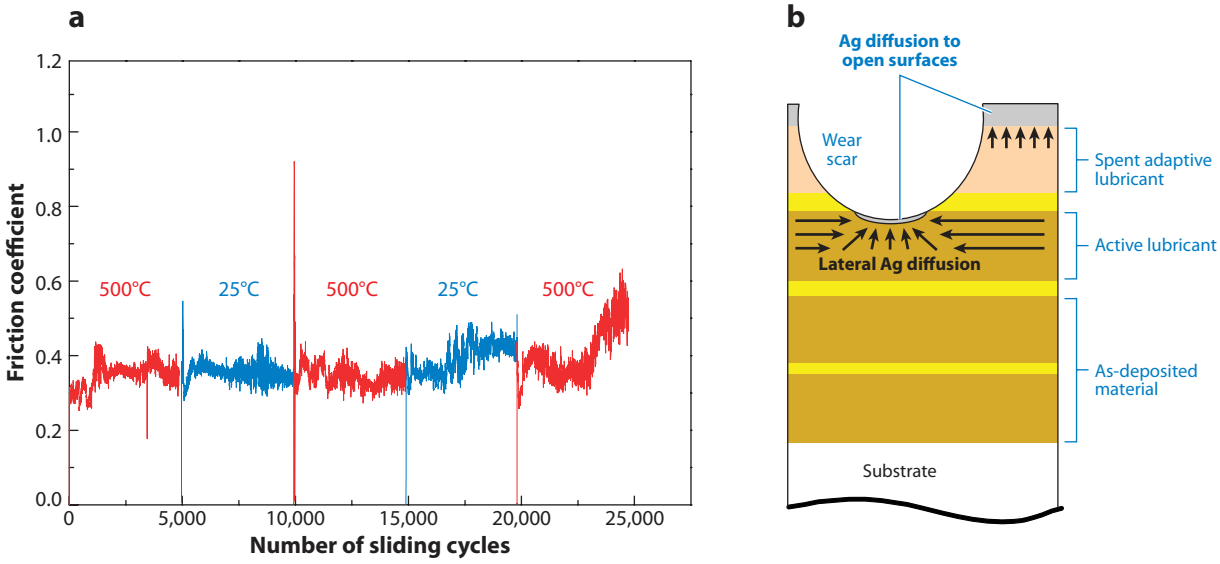

Figure 7

Friction measurements over two 500–25°C thermal cycles of 5000 sliding cycles each. Examination of the coatings after one thermal cycle (as shown on the friction trace) revealed that two adaptive lubricant layers were worn away, as suggested by the schematic on the right. Redrawn from Reference 152; used with permission from the publisher.

the silver-depleted YSZ-Mo coating rapidly wore away after cooling room temperature, exposing another chemically homogeneous adaptive coating layer buried beneath the diffusion barrier, which performed just as the as-deposited coating did at room temperature. This concept was demonstrated most recently in a seven-layer coating with four adaptive layers separated by TiN diffusion barriers (152). The coating endured two thermal cycles; one lubricant layer was consumed during each phase of the thermal cycling (**Figure 7**). This relationship between the number of thermal cycles and adaptive coating layers is currently being explored further.

These multilayer coatings lend themselves to the incorporation of sensor layers to allow in situ measurement of wear, and a warning prior to failure as diffusion barrier materials doped with rare-earth elements that fluoresce with a characteristic spectra can be placed at known thicknesses and at the film/substrate interface (153). If the worn area is illuminated with a laser, the spectrum of scattered light can be monitored to detect the exposure of the buried, rare-earth doped materials that give off distinctive and intense spectra, allowing a truly smart, reversibly adaptive, wear-resistant system.

CONCLUSIONS

Chameleon coatings, which exhibit automatic structural and chemical adaptations to the ambient environment, have been established as a means of reducing friction and wear over broad ranges of cycled environmental conditions, promoting aerospace innovations that were previously inhibited by a lack of available lubricants capable of operating in the anticipated extreme environments. Modern materials characterization techniques, such as in situ electron microscopy and high-energy X-ray diffractometry, have provided invaluable insights into fundamental mechanistic questions left unanswered for decades owing to the nature of tribological studies, in which the necessary information often lies within several atomic layers of a buried interface—certainly a

challenging region to characterize. Applications demanding expansion of the current temperature range beyond 25–800°C and increased numbers of thermal cycles are currently driving further research in adaptive nanocomposites. Although we are some time away from finding cans of lubricant delivering MoS_2-in-vacuum-like performance (for which millions of cycles without failure are commonplace) throughout cycled temperature and humidity extremes at the hardware store, accelerated progress is being made in this area with advances in instrumentation and methods currently in use to characterize adaptive lubrication and to expand the current limits in order to meet the demands of future aerospace applications.

SUMMARY POINTS

1. Solid lubrication is necessary in many space applications and at elevated temperatures.
2. Common solid lubricants have strong environmental sensitivity and can be used within only a narrow range of conditions.
3. Incorporating multiple solid lubricants that are well-suited for different environments in a hard matrix can yield reversible surface chemistry and morphology during the wear process, resulting in lubrication throughout a broader range of ambient environments.
4. If the lubricant inclusions are nanoscopic, the hardness and toughness of the composite lubricant materials can be increased, which can be useful for reducing both friction and wear.
5. Consideration of lubricant-lubricant and lubricant-environment interactions is a tool that can increase the range of operating parameters for composite solid-lubricant coatings.
6. Temperature-adaptive composite materials exhibiting diffusion-based and oxidation-based mechanisms can be used over multiple thermal cycles in microlaminate architectures, in which diffusion barrier layers separate volumes of solid lubricant.

DISCLOSURE STATEMENT

The authors are not aware of any biases that might be perceived as affecting the objectivity of this review.

LITERATURE CITED

1. Chromik RR, Baker CC, Voevodin AA, Wahl KJ. 2007. In situ tribometry of solid lubricant nanocomposite coatings. *Wear* 262:1239–52
2. Erdemir A. 2001. Solid lubricants and self-lubricating films. In *Modern Tribology Handbook, Vol. 2: Materials, Coatings and Industrial Applications*, ed. B Bhushan, pp. 787–818. Boca Raton, FL: CRC Press
3. Zabinski JS, Prasad SV, McDevitt NT. 1996. Advanced solid lubricant coatings for aerospace systems. *Proc. NATO/AGARD Tribol. Aerosp. Syst. Specialist Meet., 82nd*, pp. 1–12. London: NATO
4. Hilton MR, Fleischauer PD. 1992. Applications of solid lubricant films in spacecraft. *Surf. Coat. Technol.* 54/55:435–41
5. Todd MJ. 1982. Solid lubrication of ball bearings for spacecraft mechanisms. *Tribol. Int.* 15:331–37
6. Gschwender LJ, Nelson L, Snyder J, Fultz GW, Saba CS. 2001. Advanced high-temperature air force turbine engine oil program. In *Turbine Lubrication in the 21st Century*, ed. WR Herguth, TM Warne, ASTM STP 1407, pp. 17–24. West Conshohocken, PA: Am. Soc. Test. Mater.
7. Bowden FP, Tabor D. 1986. *The Friction and Lubrication of Solids*. New York: Oxford Univ. Press
8. Singer IL. 1989. Solid lubricating films for extreme environments. *Mater. Res. Soc. Symp. Proc.* 140:215–26

9. Sliney HE, Strom TN, Allen GP. 1963. Fluoride solid lubricants for extreme temperatures and corrosive environments. *ASLE Trans.* 8:307–22
10. Singer IL, Fayeulle S, Ehni PD. 1996. Wear behavior of triode-sputtered MoS_2 coatings in dry sliding contact with steel and ceramics. *Wear* 195:7–20
11. Erdemir A. 2004. Design criteria for superlubricity in carbon films and related microstructures. *Tribol. Int.* 37:577–83
12. Singer IL, Dvorak SD, Wahl KJ, Scharf TW. 2003. Role of third bodies in friction and wear of protective coatings. *J. Vac. Sci. Technol. A* 21:S232–40
13. Wahl KJ, Singer IL. 1995. Quantification of a lubricant transfer process that enhances the sliding life of a MoS_2 coating. *Tribol. Lett.* 1:59–66
14. Martin JM, Pascal H, Donnet C, Le Mogne Th, Loubet JL, Epicer Th. 1994. Superlubricity of MoS_2: crystal orientation mechansims. *Surf. Coat. Technol.* 68/69:427–32
15. Buck V. 1983. Morphological properties of sputtered MoS_2 films. *Wear* 91:281–88
16. Hilton MR, Bauer R, Fleischauer PD. 1990. Tribological performance and deformation of sputter-deposited MoS_2 solid lubricant films during sliding wear and indentation contact. *Thin Solid Films* 188:219–36
17. Jamison WE, Cosgrove SL. 1971. Friction characteristics of transition metal disulfides and diselenides. *ASLE Trans.* 14:62–72
18. Spalvins T. 1987. A review of recent advances in solid film lubrication. *J. Vac. Sci. Technol. A* 5:212–19
19. Gardos MN. 1988. The synergistic effects of graphite on the friction and wear of MoS_2 films in air. *Tribol. Trans.* 31:214–27
20. Moser J, Levy F. 1993. Crystal reorientation and wear mechanisms in MoS_2 lubricating thin films investigated by TEM. *J. Mater. Res.* 8:206–13
21. Spirko JA, Neiman ML, Oelker AM, Klier K. 2003. Electronic structure and reactivity of defect MoS_2 I. Relative stabilities of clusters and edges, and electronic surface states. *Surf. Sci.* 542:192–204
22. Spalvins T. 1980. Tribological properties of sputtered MoS_2 films in relation to film morphology. *Thin Solid Films* 73:291–97
23. Spalvins T. 1984. Frictional and morphological properties of Au-MoS_2 films sputtered from a compact target. *Thin Solid Films* 118:375–84
24. **Hu JJ, Wheeler R, Zabinski JS, Shade PA, Shiveley A, Voevodin AA. 2008. Transmission electron microscopy analysis of Mo-W-S-Se film sliding contact obtained by using focused ion beam microscope and in situ microtribometer. *Tribol. Lett.* 32:49–57**
25. Donnet C, Le Mogne Th, Martin JM. 1993. Superlow friction of oxygen-free MoS_2 coatings in ultrahigh vacuum. *Surf. Coat. Technol.* 62:406–11
26. Lauwerens W, Wang J, Navratil J, Wieers E, D'haen J, et al. 2000. Humidity resistant MoS_2 films prepared by pulsed magnetron sputtering. *Surf. Coat. Technol.* 131:216–21
27. Muratore C, Voevodin AA. 2008. Control of MoS_2 basal plane orientation in pulsed magnetron discharges. *Thin Solid Films*. In press
28. Roberts EW, Price WB. 1995. Advances in molybdenum disulphide film technology for space applications. *Proc. Eur. Space Mech. Tribol. Symp., 6th*, pp. 273–78. Zurich: Eur. Space Agency
29. Stupp BC. 1981. Synergistic effects of metals cosputtered with MoS_2. *Thin Solid Films* 84:257–66
30. Wahl KJ, Seitzman LE, Bolster RN, Singer IL. 1995. Low friction, high-endurance, ion-beam deposited Pb-Mo-S coatings. *Surf. Coat. Technol.* 73:152–59
31. Niederhauser P, Hintermann HE, Maillat M. 1983. Moisture-resistant MoS_2-based composite lubricant films. *Thin Solid Films* 108:209–18
32. Zabinski JS, Donley MS, Walck SD, Schneider TR, McDevitt NT. 1995. The effects of dopants on the chemistry and tribology of sputter-deposited MoS_2 films. *Tribol. Trans.* 38:894–904
33. Zabinski JS, Bultman JE, Sanders JH, Hu JJ. 2006. Multi-environmental lubrication performance and lubrication mechanism of $MoS_2/Sb_2O_3/C$ composite films. *Tribol. Lett.* 23:155–63
34. Voevodin AA, Zabinski JS. 2006. Laser surface texturing for adaptive solid lubrication. *Wear* 261:1285–92
35. **Hamilton MA, Alvarez LA, Mauntler NA, Argibay N, Colbert R, et al. 2008. A possible link between macroscopic wear and temperature dependent friction behaviors of MoS_2 coatings. *Tribol. Lett.* 32:91–98**

24. Observed atomic-scale phenomena through an intact interfacial contact. This method will provide answers to many fundamental tribological questions.

35. Measurements of surface topography during wear tests provided insight into environmental sensitivity of solid lubricants and steady-state wear rates.

36. Scharf TW, Prasad SV, Dugger MT, Kotula PG, Goeke RS, Grubbs RK. 2006. Growth, structure, and tribological behavior of atomic layer-deposited tungsten disulphide solid lubricant coatings with applications to MEMS. *Acta Mater.* 54:4731–43
37. Fleischauer PD. 1984. Effects of crystallite orientation on environmental stability and lubrication properties of sputtered MoS_2 thin films. *ASLE Trans.* 27:82–88
38. Hu JJ, Zabinski JS, Bultman JE, Sanders JH, Voevodin AA. 2006. Structure characterization of pulsed laser deposited MoS_x-WSe_y composite films of tribological interests. *Tribol. Lett.* 24:127–35
39. Chhowalla M, Amaratunga GAJ. 2000. Thin films of fullerene-like MoS_2 nanoparticles with ultralow friction and wear. *Nature* 407:164–67
40. Bragg WH. 1928. *An Introduction to Crystal Analysis*. London: Bell. 64 pp.
41. Ramadanoff D, Glass SW. 1944. High altitude brush problem. *Trans. AIEE* 63:825–29
42. Holm R. 1946. *Electrical Contacts*. Stockholm: Hugo Gebers. 193 pp.
43. Savage RH. 1947. Graphite lubrication. *J. Appl. Phys.* 19:1–10
44. Dresselhaus MS, Dresselhaus G. 1981. Intercalation compound of graphite. *Adv. Phys.* 30:139–47
45. Gardos MN. 1994. Tribology and wear behavior of diamond. In *Synthetic Diamond: Emerging CVD Science and Technology*, ed. KE Spear, J Dismukes, pp. 419–503. New York: John Wiley and Sons
46. Rowe GW. 1960. Some observations on the frictional behavior of boron nitride and of graphite. *Wear* 3:274–85
47. Rudorff W. 1941. The solution of bromine in the crystal lattice of graphite. Bromine graphite. *Z. Anorg. Chem.* 245:383–90
48. Yen BK, Schwickert BE, Toney MF. 2004. Origin of low-friction behavior in graphite investigated by surface X-ray diffraction. *Appl. Phys. Lett.* 84:4702–4
49. Deacon RF, Goodman JF. 1958. Lubrication by lamellar solids. *Proc. R. Soc. London Ser. A* 243:464–82
50. Skinner J, Gane N, Tabor D. 1971. The microfriction of graphite. *Nature* 232:605
51. Morelli DT, Beetz CP, Perry TA. 2008. Thermal conductivity of synthetic diamond films. *J. Appl. Phys.* 64:3063–66
52. Ghosh S, Calizo I, Tweldebrhan D, Pokatilov EP, Nika DL, et al. 2008. Extremely high thermal conductivity of graphene: prospects for thermal managment applications in nanoelectronic circuits. *Appl. Phys. Lett.* 92:151911
53. Berber S, Kwon YK, Tomanek D. 2000. Unusually high thermal conductivity of carbon nanotubes. *Phys. Rev. Lett.* 84:4613–16
54. Voevodin AA, Jones JJ, Zabinski JS, Czigany ZS, Hultman L. 2002. Growth and structure of fullerene-like CN_x thin films produced by pulsed laser ablation of graphite in nitrogen. *J. Appl. Phys.* 92:4980–88
55. Cao A, Dickrell PL, Sawyer WG, Ghasemi-Nejhad NG, Ajayan PM. 2005. Super-compressible foamlike carbon nanotube films. *Science* 310:1307–10
56. Collins CB, Davanloo F, Lee TJ, Park H, You JH. 1993. Noncrystalline films with the chemistry, bonding, and properties of diamond. *J. Vac. Sci. Technol. B* 11:1936–41
57. Treacy MMJ, Ebbesen TW, Gibson JM. 1996. Exceptionally high Young's modulus observed for individual carbon nanotubes. *Nature* 381:678–80
58. Kolmogorov AN, Crespi VH. 2000. Smoothest bearings: interlayer sliding in multiwalled carbon nanotubes. *Phys. Rev. Lett.* 85:4727–30
59. Neidhardt J, Hultman L. 2007. Beyond-C_3N_4–fullerene-like carbon nitride: a promising coating material. *J. Vac. Sci. Technol. A* 25:633–44
60. Angus JC, Hayman CC. 1988. Low-pressure, metastable growth of diamond and "diamondlike" phases. *Science* 19:913–21
61. Gardos MN. 1998. Tribological fundamentals of polycrystalline diamond films. *Surf. Coat. Technol.* 113:183–200
62. Grierson DS, Carpick RW. 2007. Nanotribology of carbon-based materials. *Nanotoday* 2:12–21
63. Hirano M, Shinjo K. 1990. Atomistic locking and friction. *Phys. Rev. B* 41:11837–51
64. Hirano M, Shinjo K, Kaneko R, Murata Y. 1991. Anisotropy of frictional forces in muscovite mica. *Appl. Phys. Lett.* 90:2642–45
65. Dienwiebel M, Verhoeven GS, Pradeep N, Frenken WM, Heimberg JA, Zandbergen HW. 2004. Superlubricity of graphite. *Phys. Rev. Lett.* 92:126101

66. Mate CM, McClelland GM, Erlandsson R, Chiang S. 1987. Atomic-scale friction of a tungsten tip on a graphite surface. *Phys. Rev. Lett.* 59:1942–45
67. Merkle AP, Marks LD. 2007. Friction in full view. *Appl. Phys. Lett.* 90:064101
68. Ferrari AC, Robertson J. 2000. Interpretation of Raman spectra of disordered and amorphous carbon. *Phys. Rev. B* 61:14095–107
69. Mucha JA, Flamm DL, Ibbotson DE. 1989. On the role of oxygen and hydrogen in diamond-forming discharges. *J. Appl. Phys.* 65:3448–52
70. Cuomo JJ, Doyle JP, Bruley J, Liu JC. 1991. Sputter deposition of dense diamond-like carbon films at low temperature. *Appl. Phys. Lett.* 58:466–68
71. Cuomo JJ, Pappas DL, Bruley J, Doyle JP, Saenger KL. 1991. Vapor deposition processes for amorphous carbon films with sp^3 fractions approaching diamond. *J. Appl. Phys.* 70:1706–10
72. Pappas DL, Saenger KL, Bruley J, Krakow W, Cuomo JJ, et al. 1992. Pulsed laser deposition of diamond-like carbon films. *J. Appl. Phys.* 71:5675–84
73. Erdemir A, Donnet C. 2001. Tribology of diamond-like carbon and related films. In *Modern Tribology Handbook*, *Vol. 2: Materials*, *Coatings and Industrial Applications*, ed. B Bhushan, pp. 871–903. Boca Raton, FL: CRC Press
74. Clark WT, Lancaster JK. 1963. Breakdown and surface fatigue of carbon during repeated sliding. *Wear* 6:467–82
75. Liu Y, Erdemir A, Meletis EI. 1996. An investigation of the relationship between graphitization and frictional behavior of DLC coatings. *Surf. Coat. Technol.* 86–87:564–68
76. Voevodin AA, Phelps AW, Zabinski JS, Donley MS. 1996. Friction induced phase transformation of pulsed laser deposited diamond-like carbon. *Diamond Relat. Mater.* 5:1264–69
77. Miyake S, Takahashi S, Wantanabe I, Yoshihara H. 1987. Friction and wear behavior of hard carbon films. *ASLE Trans.* 30:121–28
78. Yun X, Bogy DB, Bhatia CS. 1997. Tribolchemical study of hydrogenated carbon coatings with different hydrogen content levels in ultra high vacuum. *J. Tribol.* 119:437–42
79. Le Huu T, Zaidi H, Paulmier D. 1995. Lubricating properties of diamond-like coating. *Wear* 181–183:766–70
80. Zaidi H, Le Huu T, Paulmier D. 1994. Tribological behavior of hard carbon coatings deposited on steel substrates by plasma-assisted chemical vapour deposition. *Diamond Relat. Mater.* 3:1028–33
81. Ronkainen H, Varjus S, Koskinen J, Holmberg K. 2001. Differentiating the tribological performance of hydrogenated and hydrogen-free DLC coatings. *Wear* 249:260–66
82. Erdemir A, Eryilmaz OL, Fenske G. 2000. Synthesis of diamondlike carbon films with superlow friction and wear properties. *J. Vac. Sci. Technol. A* 18:1987–92
83. Johnson JA, Woodford JB, Rajput D, Kolesnikov AI, Schlauter JA, et al. 2008. Carbon-hydrogen bonding in near-frictionless carbon. *Appl. Phys. Lett.* 93:131911
84. Eryilmaz OL, Erdemir A. 2007. Surface analytical investigation of nearly-frictionless carbon films after tests in dry and humid nitrogen. *Surf. Coat. Technol.* 201:7401–7
85. Sliney HE. 1982. Solid lubricant materials for high temperatures—a review. *Tribol. Int.* Oct.:303–14
86. Arnell RD, Soliman A. 1978. The effects of speed, film thickness and substrate surface roughness on the friction and wear of soft metal films in ultrahigh vacuum. *Thin Solid Films* 53:333–41
87. Sliney HE. 1985. The use of silver in self-lubricating coaings for extreme temperatures. *ASLE Trans.* 29:370–76
88. Magneli A. 1953. Structures of the ReO_x-type with recurrent dislocations of homologous series of molybdenum and tungsten oxides. *Acta. Crystallogr.* 6:495–500
89. Gardos MN, Hong H, Winer WO. 1990. The effect of anion vacancies on the tribological properties of rutile (TiO_{2x}), part II: experimental evidence. *Tribol. Trans.* 36:209–20
90. Peterson MB, Li SZ, Murray SF. 1994. Wear-resisting oxide films for 900°C. *Rep. 20082401*, Argonne Natl. Lab., Argonne, IL
91. Peterson MB, Murray SF, Florek JJ. 1959. Consideration of lubricants for temperatures above 1000 F. *ASLE Trans.* 2:225–34
92. Erdemir A. 2000. A crystal-chemical approach to lubrication by solid oxides. *Tribol. Lett.* 8:97–102

91. Examination of friction and wear results for many materials at high temperature provides a guide for selecting high-temperature lubricants.

93. Murray SF, Calabrese SJ. 1993. Effect of solid lubricants on low speed sliding behavior of silicon nitride at temperatures to 800°C. *Lubr. Eng.* 49:955–64
94. John PJ, Prasad SV, Voevodin AA, Zabinski JS. 1998. Calcium sulfate as a high temperature solid lubricant. *Wear* 219:155–61
95. Sliney HE. 1979. Wide temperature spectrum self-lubrication coatings prepared by plasma spraying. *Thin Solid Films* 64:211–17
96. DellaCorte C. 1996. The effect of counterface on the tribological performance of a high temperature solid lubricant composite from 25 to 650°C. *Surf. Coat. Technol.* 86–87:486–92
97. Sliney HE, Waters WJ, Soltis R. 1997. MS212—a homogeneous sputtered solid lubricant coating for use to 800°C. *Rep. NASA Tech. Memo. 107437*, NASA Lewis Research Center, Cleveland
98. Pauleau Y, Juliet P, Gras R. 1997. Friction coefficient and wear rate of sputter-deposited thin films and plasma-sprayed thick coatings at high temperatures in room air. *Wear* 210:326–32
99. Koehler JS. 1970. Attempt to design a strong solid. *Phys. Rev. B* 2:547–51
100. Palatnik LS, Il'inskii AI. 1964. Stabilization of high-strength vacuum-deposited films. *Dokl. Sov. Phys. Tech. Phys.* 9:93–94
101. Palatnik LS, Il'inskii AI, Sapelkin NP. 1967. Strength of multilayered vacuum condensates. *Sov. Phys. Solid State* 8:2016–17
102. Holleck H, Schulz H. 1987. Advanced layer material constitution. *Thin Solid Films* 153:11–17
103. Jankowski AF. 1988. Modelling the supermodulus effect in metallic multilayers. *J. Phys. F* 18:413–27
104. Kato M, Mori T, Schwartz LH. 1980. Hardening by spinodal modulated structure. *Acta Metall.* 28:285–90
105. Chu X, Barnett SA. 1995. A model of superlattice yield stress and hardness enhancements. *Mater. Res. Soc. Symp. Proc.* 382:291–96
106. Holleck H, Schier V. 1995. Multilayer PVD coatings for wear protection. *Surf. Coat. Technol.* 76–77:328–36
107. Sproul WD. 1994. Multilayer, multicomponent, and multiphase physical vapor deposition coatings for enhanced performance. *J. Vac. Sci. Technol. A* 12:1595–601
108. Veprek S. 1999. The search for novel, superhard materials. *J. Vac. Sci. Technol. A* 17:2401–20
109. Veprek S, Reiprich S. 1995. A concept for the design of novel superhard coatings. *Thin Solid Films* 268:64–71
110. Veprek S, Niederhofer A, Moto K, Bolom T, Mannling H-D, et al. 2000. Composition, nanostructure and origin of the ultrahardness in nc-TiN/a-Si_3N_4 and nc-$TiSi_2$ nanocomposites with $H_V = 80$ to $\geq$105 GPa. *Surf. Coat. Technol.* 133–134:152–59
111. Veprek S, Argon AS. 2001. Mechanical properties of superhard nanocomposites. *Surf. Coatings Technol.* 146–147:175–82
112. Delplancke-Ogletree M-P, Monteiro OR. 1997. Deposition of titanium carbide films from mixed carbon and titanium plasma streams. *J. Vac. Sci. Technol. A* 15:1943–50
113. Voevodin AA, O'Neil JP, Prasad SV, Zabinski JS. 1997. Nanocrystalline carbide/amorphous carbon composites. *J. Appl. Phys.* 82:855–58
114. Voevodin AA, Zabinski JS, Muratore C. 2005. Recent advances in hard, tough, and low friction nanocomposite coatings. *Tsinghua Sci. Technol.* 10:665–79
115. Lyubimov VV, Voevodin AA, Yerokhin AL, Timofeev YS, Arkhipov IK. 1992. Development and testing of multilayer PVD-coatings for piston rings. *Surf. Coat. Technol.* 52:145–51
116. Voevodin AA, Walck SD, Zabinski JS. 1997. Architecture of multilayer nanocomposite coatings with superhard diamond-like carbon layers for wear protection at high contact loads. *Wear* 203–204:516–27
117. Fella R, Holleck H, Schulz H. 1988. Preparation and properties of WC-TiC-TiN gradient coatings. *Surf. Coat. Technol.* 36:257–64
118. Voevodin AA, Capano MA, Laube SJP, Donley MS, Zabinski JS. 1997. Design of a Ti/TiC/DLC functionally gradient coating based on studies of structural transitions in Ti-C films. *Thin Solid Films* 298:107–15
119. Voevodin AA, Zabinski JS. 2000. Supertough wear resistant coatings with 'chameleon' surface adaptation. *Thin Solid Films* 370:223–31

95. Outlines the development of the first solid-lubricant material to provide lubrication over a broad temperature range.

120. Voevodin A, Jones JG, Hu JJ, Fitz TA, Zabinski JS. 2001. Growth and structural characterization of yttria stabilized zirconia-gold nanocomposite films with improved toughness. *Thin Solid Films* 401:187–95
121. Donley MS, Zabinski JS. 1996. Tribological coatings. In *Pulsed Laser Deposition of Thin Films*, ed. D Chrisey, G Hubler, pp. 431–53. New York: Wiley
122. Zabinski JS, Donley MS, Dyhouse VJ, McDevitt NT. 1992. Chemical and tribological characterization of PbO-MoS_2 films grown by pulsed laser deposition. *Thin Solid Films* 214:156–63
123. Zabinski JS, Day AE, Donley MS, DellaCorte C, McDevitt NT. 1996. Synthesis and characterization of a high-temperature oxide lubricant. *J. Mater. Sci.* 29:5875–79
124. Walck SD, Zabinski JS, McDevitt NT, Bultman JE. 1997. Characterization of air-annealed pulsed laser deposited ZnO-WS_2 solid film lubricants by transmission electron microscopy. *Thin Solid Films* 305:130–43
125. Wahl KJ, Seitzman LE, Bolster RN, Singer IL, Peterson MB. 1997. Ion-beam deposited Cu-Mo coatings as high temperature solid lubricants. *Surf. Coat. Technol.* 89:245–51
126. Gulbinski W, Suszko T. 2006. Thin films of MoO_3-Ag_2O binary oxides—the high temperature lubricants. *Wear* 261:867–73
127. Voevodin AA, O'Neil JP, Zabinski JS. 1999. WC/DLC/WS_2 nanocomposite coatings for aerospace tribology. *Tribol. Lett.* 6:75–78
128. Voevodin AA, O'Neil JP, Zabinski JS. 1999. Nanocomposite tribological coatings for aerospace applications. *Surf. Coat. Technol.* 116–119:36–45
129. Miyoshi K, Wheeler DR, Zabinski JS. 1996. Surface chemistry, friction, and wear properties of untreated and laser-annealed surfaces of pulsed-laser deposited WS_2 coatings. *Rep. NASA TM-107342*, NASA Lewis Research Center, Cleveland
130. Voevodin AA, Hu JJ, Fitz TA, Zabinski JS. 2002. Nanocomposite tribological coatings with chameleon friction surface adaptation. *J. Vac. Sci. Technol. A* 20:1434–44
131. Voevodin AA. 2005. Nanocomposite and nanostructured tribological materials for space applications. *Compos. Sci. Technol.* 65:741–48
132. Baker CC, Hu JJ, Voevodin AA. 2006. Preparation of Al_2O_3/DLC/Au/MoS_2 chameleon coatings for space and ambient environments. *Surf. Coat. Technol.* 201:4224–29
133. Wu J-H, Sanghavi M, Sanders JH, Voevodin AA, Zabinski JS, Rigney DA. 2003. Sliding behavior of multifunctional composite coatings based on diamond-like carbon. *Wear* 255:859–68
134. Wu J-H, Rigney DA, Falk ML, Sanders JH, Voevodin AA, Zabinski JS. 2004. Tribological behavior of WC/DLC/WS_2 nanocomposite coatings. *Surf. Coat. Technol.* 188–189:605–11
135. Scharf TW, Singer IL. 2003. Thickness of diamond-like carbon coatings quatified with Raman spectroscopy. *Thin Solid Films* 440:138–44
136. Voevodin AA, Hu JJ, Fitz TA, Zabinski JS. 2001. Tribological properties of adaptive nanocomposite coatings made of yttria stabilized zirconia and gold. *Surf. Coat. Technol.* 146–147:351–56
137. Endrino JL, Nainaparampil JJ, Krzanowski JE. 2002. Microstructure and vacuum tribology studies of TiC-Ag composite coatings deposited by pulsed laser deposition. *Surf. Coat. Technol.* 157:95–102
138. Muratore C, Voevodin AA, Hu JJ, Zabinski JS. 2006. Tribology of adaptive nanocomposite yttria-stabilized zirconia coatings containing silver and molybdenum. *Wear* 261:797–805
139. Kutschej K, Mitterer C, Mulligan CP, Gall D. 2006. High temperature tribological behavior of CrN-Ag self-lubricating coatings. *Adv. Eng. Mater.* 8:1125–29
140. Mulligan CP, Gall D. 2005. CrN-Ag self-lubricating hard coatings. *Surf. Coat. Technol.* 200:1495–500
141. Hu JJ, Muratore C, Voevodin AA. 2007. Silver diffusion and high-temperature lubrication mechanisms of YSZ-Ag-Mo based nanocomposite coatings. *Compos. Sci. Technol.* 67:336–47
142. Muratore C, Hu JJ, Voevodin AA. 2007. Adaptive nanocomposite coatings with a titanium nitride diffusion barrier mask for high-temperature tribological applications. *Thin Solid Films* 515:3638–43
143. Kostenbauer H, Fontalvo GA, Mitterer C, Keckes J. 2008. Tribological properties of TiN/Ag nanocomposite coatings. *Tribol. Lett.* 30:53–60
144. Knotek O, Bohmer M, Leyendecker T. 1986. On structure and properties of sputtered Ti and Al based hard compound films. *J. Vac. Sci. Technol. A* 4:2695–700
145. Mayrhofer PH, Horling A, Karlsson L, Sjolen J, Larsson T, Hultman L. 2003. Self-organized nanostructurs in the Ti-Al-N system. *Appl. Phys. Lett.* 83:2049–51

122. Combined high- and low-temperature lubricants with the expectation of double-oxide formation at elevated temperature for low friction at mid-range temperatures.

127. First report of a hard, tough, humidity-adaptive nanocomposite coating.

146. Mayrhofer PH, Hovesepian PEh, Mitterer C, Munz W-D. 2004. Calorimetric evidence for frictional self-adaptation of TiAlN/VN superlattice coatings. *Surf. Coat. Technol.* 177–178:341–47
147. Gassner G, Mayrhofer PH, Kutschej K, Mitterer C, Kathrein M. 2006. Magneli phase formation of PVD Mo-N and W-N coatings. *Surf. Coat. Technol.* 201:3335–41
148. Muratore C, Voevodin AA. 2006. Molybdenum disulfide as a lubricant and catalyst in adaptive nanocomposite coatings. *Surf. Coat. Technol.* 201:4125–30
149. Aouadi SM, Paudel Y, Luster B, Stadler S, Muratore C, et al. 2008. Adaptive Mo_2N/MoS_2/Ag nanocomposite coatings for aerospace applications. *Tribol. Lett.* 29:95–103
150. Gupta S, Filimonov D, Palanisamy T, El-Raghy T, Barsoum MW. 2007. Ta_2AlC and Cr_2AlC Ag-based composites—new solid lubricant materials for use over a wide temperature range against Ni-based superalloys and alumina. *Wear* 262:1479–89
151. Paudel Y, Basnyat P, Aouadi SM, Ge Q, Muratore C, Voevodin AA. 2008. *Surf. Coat. Technol*. In press
152. Muratore C, Hu JJ, Voevodin AA. 2008. Tribological coatings for lubrication over multiple thermal cycles. *Surf. Coat. Technol.* 203:957–62
153. Muratore C, Clarke DR, Jones JG, Voevodin AA. 2008. Smart tribological coatings with wear sensing capability. *Wear* 265:913–20

148. Revealed the lowest friction obtained from 25°C to 700°C in an adaptive nanocomposite coating employing all chameleon concepts.

152. Demonstration of diffusion barriers to allow adaptive behavior over multiple thermal cycles.